molecular pharmaceutics

Article

Cite This: Mol. Pharmaceutics 2018, 15, 5031−5045

pubs.acs.org/molecularpharmaceutics

Imatinib-Loaded Micelles of Hyaluronic Acid Derivatives for Potential Treatment of Neovascular Ocular Diseases

Flavia Bongiovì,[†] Calogero Fiorica,[†] Fabio S. Palumbo,[†] Giulia Di Prima,[†,§] Gaetano Giammona,[†,‡] and Giovanna Pitarresi*[,†]

[†]Dipartimento di Scienze e Tecnologie Biologiche Chimiche e Farmaceutiche (STEBICEF), Università degli Studi di Palermo, Via Archirafi 32, 90123 Palermo, Italy

[‡]Institute of Biophysics at Palermo, Italian National Research Council, Via Ugo La Malfa 153, 90146 Palermo, Italy

Supporting Information

ABSTRACT: In this work, new micellar systems able to cross corneal barrier and to improve the permeation of imatinib free base were prepared and characterized. HA-EDA-C_{16}, HA-EDA-C_{16}−PEG, and HA-EDA-C_{16}−CRN micelles were synthesized starting from hyaluronic acid (HA), ethylenediamine (EDA), hexadecyl chains (C_{16}), polyethylene glycol (PEG), or L-carnitine (CRN). These nanocarriers showed optimal particle size and mucoadhesive properties. Imatinib-loaded micelles were able to interact with corneal barrier and to promote imatinib transcorneal permeation and penetration. In addition, a study was conducted to understand the *in vitro* imatinib inhibitory effect on a choroidal neovascularization process. Imatinib released from polymeric micelles was able to inhibit endothelial cell sprouting and to promote cell tube disruption.

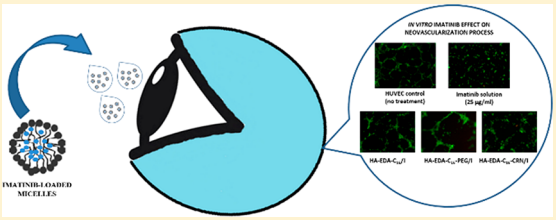

KEYWORDS: *ocular drug delivery, hyaluronic acid, polymeric micelles, imatinib, transcorneal permeation, ocular neovascular diseases*

INTRODUCTION

Neovascular ocular diseases, like age-related macular degeneration, proliferative diabetic retinopathy, and retinopathy of prematurity, share the pathophysiological mechanisms of neovascularization leading to retinal detachment and destruction of photoreceptors.[1−3] Neovascularization is a complex process where pericytes and endothelial cells proliferate and migrate to promote the formation of further blood vessels starting from existing mature vessels. This process is regulated by different growth factors including vascular endothelial growth factor (VEGF) and platelet-derived growth factor-B (PDGF-B).[4] VEGF-A, a fundamental factor of both physiological and pathological angiogenesis, is a well-known target for antiangiogenesis treatment.[5] PDGF-B, secreted by vascular endothelial cells, is a factor that attracts pericytes at the vessel formation site. PDGFR-β, a cell surface tyrosine-kinase receptor expressed on pericytes, is the main receptor for PDGF-B in the eye. The alteration of PDGF-B/PDGFR-β system can promote the formation of pericyte-deficient vessels; therefore, the anti-VEGF therapy could be more effective.[6] This allows the regression of pathological vasculature without influencing mature vessels.[7] This evidence suggests that a more potent therapy for neovascular ocular diseases can be achieved with the simultaneous use of anti-PDGF and anti-VEGF agents, with a significant reduction in blood vessel formation. In this context, small-molecule kinase inhibitors are used as antiangiogenic agents in ocular disease models since they are able to target many types of growth factor receptors.[8,9] In addition, Raimondi and colleagues reported that neuropilin 1 (NRP1) regulates angiogenesis via ABL1 and in a VEGF- and VEGFR2-independent manner; this result proposes that the ABL1 inhibition represents a new antiangiogenic treatment to complement VEGF and PDGF blockade in neovascular ocular diseases or in the growth of solid tumor.[10] Imatinib mesylate (Gleevec, formerly STI-571), a multitargeted tyrosine kinase inhibitor (TKI), is administered for molecularly targeted therapy in different types of cancer such as glomerular disease and Ph+ chronic myeloid leukemia (Ph+CML).[11] Imatinib is a small-molecule kinase inhibitor of ABL1 extensively used to suppress tumor proliferation by blocking Bcr-Abl fusion proteins expressed in the tumor cells. Imatinib selectively inhibits also the PDGF receptors (α and β) and c-Kit, but it does not inhibit other receptors or cytoplasmic tyrosine kinases.[12] In last years, different researcher groups designed various nanosystems to release imatinib free base for treatment of cancer. Gupta and colleagues prepared imatinib-loaded nanostructured lipid carriers to improve the *in vitro* and *in vivo* profile of drug.[13] Ramazani and colleagues developed imatinib-loaded poly(D,L-lactide-*co*-glycolide) (PLGA) microspheres that can allow the prolonged release of imatinib.[14] Tivozanib, axitinib, and other TKI molecules are experimentally employed to evaluate the efficacy on retinal and choroidal neovascularization.[8,15] Therefore, the aim of this study was to

Received: June 14, 2018
Revised: August 15, 2018
Accepted: September 24, 2018
Published: September 24, 2018

DOI: 10.1021/acs.molpharmaceut.8b00620
Mol. Pharmaceutics 2018, 15, 5031−5045

prepare imatinib (free base)-loaded polymeric micelles for the potential treatment of neovascular ocular diseases. Mucoadhesive polymeric micelles were obtained starting from an appropriate derivative of hyaluronic acid (HA), a natural component of vitreous body and aqueous humor. This biopolymer is able to increase the time of corneal contact of the aqueous formulations, reduce the loss of drugs, and improve their bioavailability.[16] Furthermore, HA can be chemically modified to obtain derivatives that can be used both in regenerative medicine and drug delivery fields.[17−20] In particular, the synthesis and characterization of an amphiphilic derivative of hyaluronic acid containing ethylenediamine (EDA) and hexadecyl groups (C_{16}), called HA-EDA-C_{16}, were reported here. EDA was used to insert primary amine groups on HA backbone that are useful for additional functionalization. In fact, in previous works, it was demonstrated that the presence of reactive amine groups on HA backbone allows researchers to obtain various systems for different uses.[18,21−23] In this work, HA-EDA-C_{16} derivative was used to prepare micelles through a cosolvent evaporation method. To improve drug corneal passage, the external shell of micelles was modified with corneal penetration enhancers such as PEG or L-carnitine. PEG chains on the micelle surface can act as mucoadhesion promoters because they enhance the contact time with the mucus layer of the tear film; in addition, PEGylated shells play an important role in enhancing the corneal penetration of drug-loaded micelles.[24,25] On the other hand, L-carnitine protects corneal cells from hyperosmotic stress in dry eye and retinal pigment epithelium from H_2O_2-induced oxidative damage.[26] L-Carnitine is transported into cells by OCTN1 and OCTN2 (Organic Cation Transporter System), which are on the surface of human corneal and conjunctival epithelial cells.[27,28] Therefore, L-carnitine-decorated micelles were designed as smart colloidal carriers able to promote drug absorption after administration on the ocular surface probably through OCTN interactions. Starting from HA-EDA-C_{16}, two polymeric derivatives named HA-EDA-C_{16}−PEG and HA-EDA-C_{16}−CRN were synthesized by grafting PEG (Mw of 2 kDa) or L-carnitine (CRN), respectively. Therefore, HA-EDA-C_{16}−PEG and HA-EDA-C_{16}−CRN micelles were prepared by using the cosolvent evaporation method. The mucoadhesive properties and size of these micelles were compared to data obtained for HA-EDA-C_{16} micelles. All synthesized polymeric derivatives were used to prepare imatinib-loaded micelles; the ability of these carriers to entrap and release the drug was assessed by *in vitro* analyses. Drug-loaded micelles were tested by using *in vitro* and *ex vivo* models to evaluate the imatinib permeation through a monolayer of human corneal epithelial cells and bovine cornea, respectively. Finally, an *in vitro* model of neovascularization was employed to evaluate the antiangiogenic effect of imatinib (as a solution or loaded into micelles). For this study, HUVEC and ECM (extra-cellular matrix) gel were used as an ophthalmological *in vitro* model.[29,30]

EXPERIMENTAL SECTION

Materials. All solvents and chemicals were of analytical grade. Hyaluronic acid mini (HA_{MINI}; Mw 7.3 kDa; M_w/M_n 1.63) was purchased from Biophil Italia S.P.A. Tetrabutylammonium hydroxide (TBA−OH), bis(4-nitrophenyl)-carbonate (4-NPBC), hexadecylamine (C_{16}−NH_2), O-[2-(6-oxocaproylamino)ethyl]-O′-methylpolyethylene glycol 2000 (PEG-aldehyde, PEG-CHO Mw 2 kDa), L-carnitine inner salt (CRN), Dulbecco's phosphate buffered saline pH 7.4 (DPBS), diethyl ether, chloroform ($CHCl_3$), ethanol (EtOH), tetramethylammonium chloride (TMACl), anhydrous dimethyl sulfoxide ($DMSO_A$), methanol (MeOH), picrylsulfonic acid solution (2,4,6-trinitrobenzenesulfonic acid, TNBS), methoxypolyethylene glycol amine (PEG-NH_2, Mw 2 kDa), pyrene, mucin type III (from porcine stomach) and 4-(2-hydroxyethyl)piperazine-1-ethanesulfonic acid (HEPES), Sephadex G-25, imatinib (I), N-(3-(dimethylamino)propyl)-N′-ethylcarbodiimide hydrochloride (EDC), *N*-hydroxysuccinimide (NHS), and ECM Gel from Engelbreth-Holm-Swarm murine sarcoma (EHS matrix) were purchased from Sigma-Aldrich (Italy). Ethylenediamine was purchased from Fluka (Italy). Deuterium oxide (D_2O), sodium chloride (NaCl), and sodium hydrogen carbonate ($NaHCO_3$) were purchased from Merck (Italy). Tetrahydrofuran-$_{d8}$ (THF-d_8) was purchased from VWR (Italy). Tetrahydrofuran (THF) was purchased from Alfa Aesar (Italy); AlexaFluor-NHS488 (carboxylic acid, succinimidyl ester) and Live&Dead Viability/Cytotoxicity Kit for mammalian cells were purchased from Life Technologies-Thermo Fisher Scientific (USA).

HEPES buffer pH 7.4, simulating ocular fluid, was prepared by dissolving HEPES (5.96 g) and NaCl (9 g) in 1 L of bidistilled water, with pH value adjusted with NaOH 5 M. Human corneal epithelial cells (HCEpiC) and Human umbilical vein endothelial cells (HUVEC) were purchased from ScienCell Research Laboratories (USA). Keratinocyte serum-free basal medium with bovine pituitary extract (BPE, 50 μg/mL) and recombinant human epithelial growth factor (EGF, 5 ng/mL) were used for the culture of HCEpiC and the *in vitro* experiments (Gibco−Thermo Fisher Scientific, USA). Endothelial cell growth medium (all-in-one ready-to-use) was used for the culture of HUVEC and the *in vitro* experiments (Sigma-Aldrich, Italy).

Apparatus. Proton nuclear magnetic resonance (^{1}H NMR) was performed by using a Bruker Avance II 300 spectrometer operating at 300.12 MHz. FT-IR spectra were carried out by using a Bruker Alpha instrument. Ultraviolet (UV) measurements were carried out by using a Shimadzu UV-2401PC spectrophotometer. Gel permeation chromatography (GPC) was performed by using an Agilent 1260 Infinity Multi-Detector Bio-SEC solution, as reported elsewhere.[17] GPC system was equipped with a pump system, a PolySep-GFC-P 4000 column from Phenomenex, Bio-Dual Angle LS/DLS, and RI Detector. Analyses were performed with 70% 0.025 M TMACl solution and 30% MeOH mixture as an eluent, with a flow of 0.6 mL/min and a column temperature of 35 °C ± 0.1. Pullulan standards (range 5.9−788 kDa) were used to obtain the calibration curve. Pyrene emission spectra were recorded by using a RF-5301PC spectrofluorometer (Shimadzu, Italy). Dynamic light scattering (DLS) analyses were conducted at 25 °C by using a Malvern Zetasizer Nano ZS instrument, fitted with a 532 nm laser at a fixed scattering angle of 173° (Malvern Instrument, Malvern). Drug detection was performed by using a HPLC Agilent instrument 1260 Infinity equipped with a Quaternary Pump VL G1311C and a DAD detector 1260 VL, 50 μL injector, and a computer integrating apparatus (OpenLAB CDS ChemStation Workstation). A reversed phase column Luna Phenomenex C18 (100 A size 250 × 4.60 mm^2) was employed as a stationary phase at controlled temperature (20 °C); a mobile phase of methanol was used with a flow equal to 0.8 mL/min. The wavelength of 270 nm was selected for the quantification. To obtain a calibration

DOI: 10.1021/acs.molpharmaceut.8b00620
Mol. Pharmaceutics 2018, 15, 5031−5045

curve, imatinib standard solutions were prepared in MeOH for the evaluation of drug loading and drug amount *in vitro* and *ex vivo* experiments.

Synthesis and Characterization of HA-EDA-C_{16} Derivative. Tetrabutylammonium salt of HA (HA-TBA) was produced as reported elsewhere.[22,31] One gram of HA-TBA, dissolved at 1% (w/v) in $DMSO_A$, was mixed with $DMSO_A$ containing the appropriate amount of 4-NPBC to have a molar ratio (X) between 4-NPBC and HA-TBA repeating unit, equal to 0.7. Reaction was left at 40 °C for 4 h. After this time, the temperature was increased to 60 °C and an appropriate amount of hexadecylamine ($C_{16}NH_2$), dissolved in $DMSO_A$, was added to have a molar ratio (Y) between $C_{16}NH_2$ and 4-NPBC equal to 0.3. Reaction was left at 60 °C for 20 h. After this time, temperature was decreased to 40 °C and an appropriate amount of ethylenediamine (EDA) was added to have a molar ratio (Z) between EDA and 4-NPBC equal to 2. After 3 h, 1 mL of aqueous NaCl saturated solution was added under stirring for 30 min at room temperature to exchange tetrabutylammonium with sodium. Reaction product was precipitated in EtOH and washed several times (with EtOH 90% and EtOH). Product was dried under vacuum; the yield of HA-EDA-C_{16} derivative was calculated compared to the weight of starting HA and it was equal to 81.7% ± 3.1. Derivatization degree in C_{16} (DD_{C16} mol %) was calculated by ^{1}H NMR. ^{1}H NMR (300.12 MHz, D_2O/THF-d_8 3:2 (v/v), δ): 0.99 (s, 3H, $-CH_3$ of hexadecylamine), 1.5 (br m, 28H, $-CH_2-(CH_2)_{14}-CH_3$ of hexadecylamine), 1.9 (s, 3H, $NH-CO-CH_3$ of hyaluronic acid), 3.3−4.0 (pyranosyl group of HA). The molar derivatization degree in C_{16} portions linked to HA (DD_{C16} mol %) was calculated by comparing the peak at δ 0.99 and δ 1.5, attributable to methyl and methylene groups of C_{16} chain, with the peak at δ 1.9, attributable to acetamido group of HA. The derivatization degree in pendant EDA groups linked to HA (DD_{EDA} mol %) was determined by TNBS colorimetric assay using PEG-NH_2 (Mw 2 kDa) as a standard.[22,32] The weight-average molecular weight (Mw) of HA-EDA-C_{16} derivative was determined by GPC analysis (see Apparatus). Each sample (5 mg) was dissolved in 700 μL of 0.025 M TMACl solution, and then 300 μL of methanol was added. Samples and pullulan standards were filtered through 0.45 μm and injected into GPC apparatus.

Synthesis and Characterization of HA-EDA-C_{16}−PEG Derivative. HA-EDA-C_{16} was dissolved in bidistilled water at pH 6.5 with HCl 0.1 N. An appropriate amount of PEG-aldehyde (Mw 2 kDa) was added to have a molar ratio between PEG-aldehyde and HA-EDA-C_{16} repeating unit equal to 0.1. pH value was monitored and adjusted at 6.5 with HCl 0.1 N; reaction was left at room temperature for 24 h, under stirring. Final product was purified by using dialysis bag (MWCO 3.5 kDa) against water for 3 days, and then polymer solution was freeze-dried. The yield of HA-EDA-C_{16}−PEG derivative was calculated compared to the weight of starting HA-EDA-C_{16} derivative and it was equal to 85.1% ± 2.3. Derivatization degree in PEG (DD_{PEG} mol %) was calculated by ^{1}H NMR. ^{1}H NMR (300.12 MHz, D_2O, δ): 0.99 (s, 3H, $-CH_3$ of hexadecylamine), 1.5 (br m, 28H, $-CH_2-(CH_2)_{14}-CH_3$ of hexadecylamine), 1.9 (s, 3H, $NH-CO-CH_3$ of hyaluronic acid), 3.3−4.0 (pyranosyl groups of HA), 3.6 (s, 180H, $-O-(CH_2-CH_2-O)_{45}-$ groups of PEG). The molar derivatization degree in PEG, expressed as moles of PEG portions linked per moles of HA-EDA-C_{16} repeating unit % (DD_{PEG} mol %), was calculated by comparing integral of the peak at δ 3.6, attributable to methylene groups of PEG chain, with the peak at δ 1.9, attributable to acetamido group of HA. Derivatization degree in PEG was also calculated with TNBS colorimetric assay and confirmed by FT-IR analysis (HA-EDA-C_{16}−PEG spectrum showed the C−H scissoring and bending band of PEG in the range 1450−1300 cm^{-1}, and the N−H bending band of PEG at 800 cm^{-1}). The weight-average molecular weight (Mw) of HA-EDA-C_{16}−PEG derivative was determined by GPC analysis using the conditions reported above.

Synthesis and Characterization of HA-EDA-C_{16}−CRN Derivative. To synthesize HA-EDA-C_{16}−CRN derivative, L-carnitine (CRN) was dissolved in bidistilled water at pH 5 with HCl 0.1 N. To activate carboxyl group of CRN, appropriate amounts of NHS and EDC were added to have both molar ratios between NHS and CRN and between EDC and CRN equal to 1.5. This step of activation was performed at room temperature for 4 h. Afterward, activated CRN solution was added dropwise to a HA-EDA-C_{16} aqueous solution at the concentration of 1% (w/v). The molar ratio between L-carnitine and HA-EDA-C_{16} repeating unit was equal to 0.1. The reaction was left at room temperature for 20 h under stirring. Final product was purified through a dialysis (MWCO 2 kDa) against water for 3 days, then was recovered after freeze-drying. The yield of HA-EDA-C_{16}−CRN derivative was calculated compared to the weight of the starting HA-EDA-C_{16} derivative and it was equal to 87.3% ± 3.1. Derivatization degree in CRN (DD_{CRN} mol %) was calculated by ^{1}H NMR. ^{1}H NMR (300.12 MHz, D_2O, δ): 0.99 (s, 3H,-CH_3 of hexadecylamine), 1.5 (br m, 28H, $-CH_2-(CH_2)_{14}-CH_3$ of hexadecylamine), 1.9 (s, 3H, $NH-CO-CH_3$ of hyaluronic acid), 2.8 (s, 9H, $-N^+(CH_3)_3$ of L-carnitine), 3.3−4.0 (pyranosyl groups of HA). The derivatization degree in L-carnitine, expressed as moles of CRN portions linked per moles of HA-EDA-C_{16} repetitive unit % (DD_{CRN} mol %), was calculated by comparing the peak at δ 2.8, attributable to methyl groups of L-carnitine, with the peak at δ 1.9, attributable to acetamido group of HA. Derivatization degree in CRN was also calculated by TNBS colorimetric assay. The weight-average molecular weight (Mw) of HA-EDA-C_{16}−CRN derivative was determined by GPC analysis using the conditions reported above.

Critical Aggregation Concentration (CAC) Determination by Fluorescence Spectroscopy. The critical aggregation concentration (CAC) of HA-EDA-C_{16}, HA-EDA-C_{16}−PEG, and HA-EDA-C_{16}−CRN derivatives was determined by fluorescence spectroscopy using pyrene as a fluorescence probe.[33] Briefly, 100 μL of pyrene solution (6.0×10^{-5} M) in acetone was added to a series of vials followed by evaporation to remove the acetone. Aqueous solutions of each derivative (in bidistilled water, DPBS, and HEPES buffer) with concentrations ranging from 1×10^{-4} to 2 mg/mL were added to each vial, and then samples were left overnight in orbital shaker (100 rpm) at 37 °C to equilibrate pyrene with micelles. The final concentration of pyrene in each vial was 6.0×10^{-7} M. Solutions were placed in quartz cuvettes and emission spectra were recorded. The change in pyrene intensity ratio (I_{373}/I_{384}) was plotted as a function of sample concentration (mg/mL) and the CAC value was determined.[34]

Preparation and Characterization of Empty and Drug-Loaded HA-EDA-C_{16}, HA-EDA-C_{16}−PEG, and HA-EDA-C_{16}−CRN Micelles. A cosolvent evaporation method was used to prepare drug-loaded HA-EDA-C_{16}, HA-EDA-C_{16}−

DOI: 10.1021/acs.molpharmaceut.8b00620
Mol. Pharmaceutics 2018, 15, 5031−5045

PEG, and HA-EDA-C_{16}−CRN micelles. For the drug-loaded micelles, imatinib and each polymeric derivative were dissolved in THF/H_2O 1:1 (v/v) mixture to obtain a final polymer concentration of 0.3% (w/v). The weight ratio between each derivative and drug was equal to 1:0.5 (w/w). THF was removed by evaporation under stirring (1000 rpm) at room temperature for 3 h; vacuum was applied to remove the residual organic solvent. At the end of drug loading process, the colloidal dispersion was centrifuged, filtered through a 1 μm syringe filter, and subsequently lyophilized. Empty micelles were prepared in the same manner. The values of particle size (nm), polydispersity index (PDI), and ζ-potential (mV) of all micelles were determined by DLS analysis. Each micellar dispersion (1 mg/mL), obtained by using bidistilled water, DPBS, and HEPES buffer pH 7.4 as suspending media, was analyzed in triplicate. In addition, the stability of empty and drug-loaded micelles, in terms of particle size, was evaluated in DPBS at 25 °C until 7 days (Supplemental Figure I). The amount of imatinib (I) in drug-loaded micelles was determined through HPLC. Each sample was dispersed in methanol overnight under stirring, and then it was filtered with 0.45 μm filter and analyzed by HPLC. Each analysis was performed in triplicate. The drug loading percentage (DL%) was calculated as the ratio between the weight of drug into micelles and the weight of drug plus polymer.

Preparation and Characterization of Fluorescent-Labeled HA-EDA-C_{16}, HA-EDA-C_{16}−PEG, and HA-EDA-C_{16}−CRN Micelles. Fluorescent-labeled micelles were prepared similarly as reported elsewhere.[35] Empty HA-EDA-C_{16}, HA-EDA-C_{16}−PEG, and HA-EDA-C_{16}−CRN micelles were dispersed in pH 8.3 bicarbonate buffer solution at the concentration of 10 mg/mL; pH value was adjusted to 8.3 with HCl 0.1 N. AlexaFluor-NHS_{488} (solubilized in DMSO at the concentration of 10 mg/mL) was added to the micellar dispersion considering the weight ratio between $AlexaFluor_{488}$ and micelles equal to 1:100. pH value was adjusted again to 8.3, and then the reaction was carried out at room temperature in the dark for 1 h under stirring. Final product was purified by GPC using a Sephadex G25 column. Recovered fluorescent-labeled micelles were lyophilized. The yield of HA-EDA-C_{16}−$AlexaFluor_{488}$, HA-EDA-C_{16}−PEG-$AlexaFluor_{488}$, and HA-EDA-C_{16}- CRN-$AlexaFluor_{488}$ micelles was calculated with respect to the starting weight of micelles and it was equal to 95.1% ± 0.9, 97.4% ± 1.6, and 96.8% ± 2.1, respectively. The values of particle size (nm), polydispersity index (PDI), and ζ-potential (mV) of all micelles were determined by DLS analysis. Each micellar dispersion (1 mg/mL), obtained by using bidistilled water, DPBS, and HEPES buffer pH 7.4 as suspending media, was analyzed in triplicate (Supplemental Table 1). In addition, the stability of micelles, in terms of particle size, was evaluated in DPBS at 25 °C until 7 days (Supplemental Figure II).

Mucoadhesion Studies. The mucoadhesive properties of HA-EDA-C_{16}, HA-EDA-C_{16}−PEG, and HA-EDA-C_{16}−CRN micelles were evaluated by transmittance analysis. Micelles and mucin dispersion were mixed with a ratio 1:1 (v/v) to obtain a final mucin and micelles concentration of 1 and 5 mg/mL, respectively. Each sample was incubated in orbital shaker (100 rpm) at 35 °C; at scheduled time points (from 10 to 360 min), sample transmittance was measured at 500 nm. Unmodified HA_{MINI} was used as a positive control. Obtained data were reported as transmittance %, calculated as the ratio between sample and mucin transmittance values. The decrease in transmittance % of sample demonstrated mucoadhesive properties. Each experiment was performed in six replicates.

***In Vitro* Imatinib Release Studies.** Drug release studies from HA-EDA-C_{16}/I, HA-EDA-C_{16}−PEG/I, and HA-EDA-C_{16}−CRN/I micelles were conducted at pH 7.4 in sink conditions by using the dialysis method. Each sample (total drug amount equal to 0.5 mg for each system) was dispersed in DPBS at the concentration of 1% (w/v) and placed in a dialysis bag (MWCO 1 kDa); DPBS was used as a release medium. A ratio between internal and external environment equal to 1:10 (v/v) was set. Samples were left in a thermostatic shaker (100 rpm, 37 °C); at scheduled time-points (from 10 min to 48 h), the aliquots of receiving medium (1 mL) were taken and replaced by fresh medium (1 mL). The drug amount in each sample was determined by using a UV−vis spectrophotometer (λ = 257 nm). Free drug solutions (0.025 mg/mL) and suspensions (0.5 mg/mL) in DPBS were used as a comparison. To prepare imatinib solution, drug was previously dissolved in methanol at the concentration of 2.5 mg/mL, then diluted in DPBS to obtain the final concentration of 0.025 mg/mL (residual methanol is equal to 1% v/v).

***In Vitro* Cell Viability Assay.** HCEpiC viability was evaluated after the treatment with HA-EDA-C_{16}, HA-EDA-C_{16}−PEG, and HA-EDA-C_{16}−CRN micelles. Micelles were dispersed in DPBS at the concentration of 10 mg/mL. Each stock solution was sterilized by filtration using a sterile 0.22 μm syringe membrane filter. The values of drug loading and particle size were measured before and after filtration to check the integrity of micelles. Dispersions of micelles at different concentration were prepared by dilution of the stock solution with complete cell culture medium. HCEpiC (passage 2−3) were seeded in a 96-well plate at a density of 10^5 cells/well and incubated overnight at 37 °C in a humidified atmosphere with 5% CO_2. The medium into each well was replaced by 200 μL of medium containing empty micelles, at a final concentration per well ranging between 0.01 and 0.7 mg/mL. HCEpiC viability was evaluated after 6 and 24 h of incubation by using MTS (3-(4,5-dimethylthiazol-2-yl)-5-(3-carboxymethoxyphenyl)-2-(4sulfophenyl)-2H-tetrazolium assay (CellTiter 96 AQueous One Solution Cell Proliferation, PROMEGA) following the supplier's instructions. HUVEC viability was assessed after the treatment with imatinib solution, empty micelles, or drug-loaded micelles. HUVEC (passage 6−7) were seeded in a 96-well plate at the density of 3×10^4 cells/well and incubated overnight at 37 °C in a humidified atmosphere with 5% CO_2. In the first experiment, imatinib solution was prepared in MeOH at the concentration of 10 mg/mL, and then it was diluted in complete cell culture medium in the range 0.5−125 μg/mL (residual MeOH was in the range 0.005−1.25% v/v). The medium into each well was replaced by 150 μL of imatinib solution at different concentrations or by 150 μL of complete cell culture medium with MeOH 1.25% (v/v). HUVEC viability was evaluated after 6 and 24 h of incubation by using MTS assay. In the second experiment, empty and drug-loaded HA-EDA-C_{16}, HA-EDA-C_{16}−PEG, and HA-EDA-C_{16}−CRN micelles were dispersed in DPBS at the concentration of 3 mg/mL. Each stock solution, after filtration with a sterile 0.22 μm filter, was diluted in complete cell culture medium at the concentration of 3 mg/mL. HUVEC viability was evaluated after 6 and 24 h of incubation by using MTS assay. For all experiments, the absorbance of each sample was measured using a multiwell plate reader (Tecan, Groedig, Austria) at 490 nm. Results were reported as

DOI: 10.1021/acs.molpharmaceut.8b00620
Mol. Pharmaceutics 2018, 15, 5031−5045

cell viability %, calculated as the ratio between the optical density of sample and the optical density of HCEpiC or HUVEC cultured in tissue culture polystyrene (TCPS) used as control cells.

Transcorneal Permeation Studies: *In Vitro* Transcorneal Permeation. The *in vitro* transcorneal permeation study was conducted as reported elsewhere.[17] For this study, transwell system was chosen as an experimental system which mimics the physiological corneal barrier. HCEpiC were seeded at a density of 10^5 cells/well on the top of a collagen-coated filter (0.4 μm pores −6.5 mm, 0.33 cm^2 Transwell-PTFE membrane insert, Corning); cells were grown until confluence by changing the complete cell culture medium every day.[36−38] The donor and acceptor chambers of transwell were filled with 150 μL and 650 μL of complete cell culture medium, respectively. On the day of the experiment, the medium in the donor chamber was removed and replaced by 150 μL of: (1) a fluorescent-labeled micellar dispersions in complete cell culture medium at the concentration of 2 mg/mL; (2) HA-EDA-C_{16}/I, HA-EDA-C_{16}−PEG/I, and HA-EDA-C_{16}−CRN/I micelles dispersed in complete cell culture medium; samples were dispersed in DPBS, filtered by using a 0.22 μm filter, and then diluted in complete cell culture medium to obtain a final drug concentration equal to 100 μg/mL; (3) imatinib solution (drug was previously solubilized in MeOH at 2.5 mg/mL and then it was diluted in complete cell culture medium at 0.025 mg/mL; residual MeOH was less than 1% v/v). Samples were incubated at 37 °C in a humidified atmosphere with 5% CO_2. At scheduled time intervals (from 0.25 to 6 h), aliquots (200 μL) were withdrawn from the acceptor chamber and immediately replaced by the same amount of fresh medium to maintain sink conditions. For the HA-EDA-C_{16}−AlexaFluor$_{488}$, HA-EDA-C_{16}−PEG-AlexaFluor$_{488}$, and HA-EDA-C_{16}-CRN-AlexaFluor$_{488}$ micelles, collected samples were analyzed by using spectrofluorometer (λ_{ex}, 485 nm; λ_{em}, 520 nm). For drug-loaded micelles, recovered samples were lyophilized, treated with MeOH, and then analyzed by HPLC. Results were expressed as $\mu g/cm^2$ of fluorescent-labeled micelles permeated or drug permeated as a function of incubation time (h). Each experiment was performed in triplicate.

Transcorneal Permeation Studies: *Ex Vivo* Transcorneal Permeation. The *ex vivo* transcorneal permeation study was conducted by using bovine corneas and a vertical Franz type diffusion cell, chosen as a two-compartment open model.[39] The validation of the *ex vivo* model was reported elsewhere.[17] All animal tissues were collected by Istituto Zooprofilattico della Sicilia "A. Mirri" (Palermo, Italy) following authorization of local Department of Veterinary Prevention (ASP-Palermo, Italy). Entire bovine eyeballs were immersed for 2 h in streptomycin 1% (v/v) containing DPBS; cornea was obtained by carefully detaching it from underlying iris using tweezers. Each cornea was washed in HEPES buffer pH 7.4, then used as a membrane in vertical Franz type diffusion cell (active area available for permeation equal to 1.1304 cm^2). Donor and acceptor chambers were filled with HEPES buffer and placed at 35 °C ± 0.1. After 15 min, HEPES solution was removed from donor chamber and replaced by 300 μL of (1) a fluorescent-labeled micellar dispersions in HEPES buffer at the concentration of 3 mg/mL; (2) HA-EDA-C_{16}/I, HA-EDA-C_{16}−PEG/I, and HA-EDA-C_{16}−CRN/I micelles in HEPES buffer (final drug amount in the donor chamber was equal to 150 μg); (3) imatinib solution (drug was previously solubilized in MeOH at 2.5 mg/mL and then it was diluted in HEPES at 0.025 mg/mL); and (4) imatinib suspension (0.5 mg/mL) in HEPES buffer. Volume in the acceptor chamber was equal to 4.5 mL; area available to permeation was 1.1304 cm^2. Each experiment was carried out in six replicates for 360 min under stirring (50 rpm); at scheduled time intervals (from 0.25 to 6 h), aliquots (200 μL) were withdrawn from acceptor chamber and replaced by the same volume of fresh HEPES to maintain sink conditions. In addition, imatinib amount that remains entrapped into corneal tissue at the end of the experiment was quantified. Each cornea was washed with HEPES buffer to remove the drug remained on its surface and then it was treated with 2 mL of MeOH overnight at 37 °C under stirring (300 rpm). Obtained solutions were analyzed by HPLC. For the HA-EDA-C_{16}−AlexaFluor$_{488}$, HA-EDA-C_{16}−PEG-AlexaFluor$_{488}$, and HA-EDA-C_{16}−CRN-AlexaFluor$_{488}$ micelles, collected samples were immediately analyzed by using a spectrofluorometer (λ_{ex}, 485 nm; λ_{em}, 520 nm). Other samples were lyophilized; 200 μL of MeOH was added to dissolve drug and obtained solution was analyzed by HPLC. All results were expressed as $\mu g/cm^2$ of permeated fluorescent-labeled micelles or permeated drug as a function of incubation time (h).

***In Vitro* Endothelial Cell Tube Formation Assay.** Endothelial cell tube formation was observed on ECM gel from Engelbreth-Holm-Swarm murine sarcoma (EHS matrix). Gel solidifies at 37 °C, forming a basement membrane rich in pro-angiogenic factors on top of which endothelial cells can form tubular complexes.[29] For all experiments, 75 μL of the EHS matrix were transferred to each well of a 96-well plate. Plate was incubated at room temperature at least 10 min and then incubated for 30 min at 37 °C (humidified atmosphere with 5% CO_2). In the first experiment, HUVEC suspension (75 μL) was added to an equal volume of (1) imatinib solution at the concentration in the range of 5−25 μg/mL; imatinib was previously solubilized in MeOH at the concentration of 10 mg/mL, then diluted with complete cell culture medium (residual MeOH was less than 1% v/v); (2) HA-EDA-C_{16}/I, HA-EDA-C_{16}−PEG/I, and HA-EDA-C_{16}−CRN/I micellar dispersion; samples were dispersed in DPBS (1 mg/mL), filtered with a 0.22 μm filter, and then diluted with complete cell culture medium (0.3 mg/mL) to obtain a final drug concentration of 40 μg/mL. Each prepared dispersion (cells with imatinib solution or cells with drug-loaded micelles) was added on the top of gel layer to obtain a final cell density of 3 × 10^4 cells/well. Plate was incubated at 37 °C (humidified atmosphere with 5% CO_2); endothelial cell tube formation was observed until 24 h using an optical microscope with a 10× magnification. In the second experiment, HUVEC (passage 6−7) were first seeded on the top of a thin gel layer at the density of 3 × 10^4 cells/well. After the complete tube formation occurred, cell medium was removed from each well and then 150 μL was added of imatinib solution at the concentration in the range of 5−25 μg/mL (prepared as described above) or HA-EDA-C_{16}/I, HA-EDA-C_{16}−PEG/I, HA-EDA-C_{16}−CRN/I micellar dispersion with a final drug concentration of 40 μg/mL (samples were prepared as described above). Plate was incubated at 37 °C (humidified atmosphere with 5% CO_2); the alteration of endothelial cell tube structures was observed until 24 h, using an optical microscope with a 10× magnification. At the end of experiments, when possible, Live&Dead assay was conducted following the supplier's instructions. Images were acquired using a CareZeis Axio Vert microscope with a 10× magnification.

DOI: 10.1021/acs.molpharmaceut.8b00620
Mol. Pharmaceutics 2018, 15, 5031−5045

Scheme 1. Chemical Procedure for Hyaluronic Acid (HA) Derivatization with C_{16}−NH_2 Chains and EDA Groups To Obtain HA-EDA-C_{16} Derivative, Starting from HA-TBA and Using 4-NPBC as Activating Agent

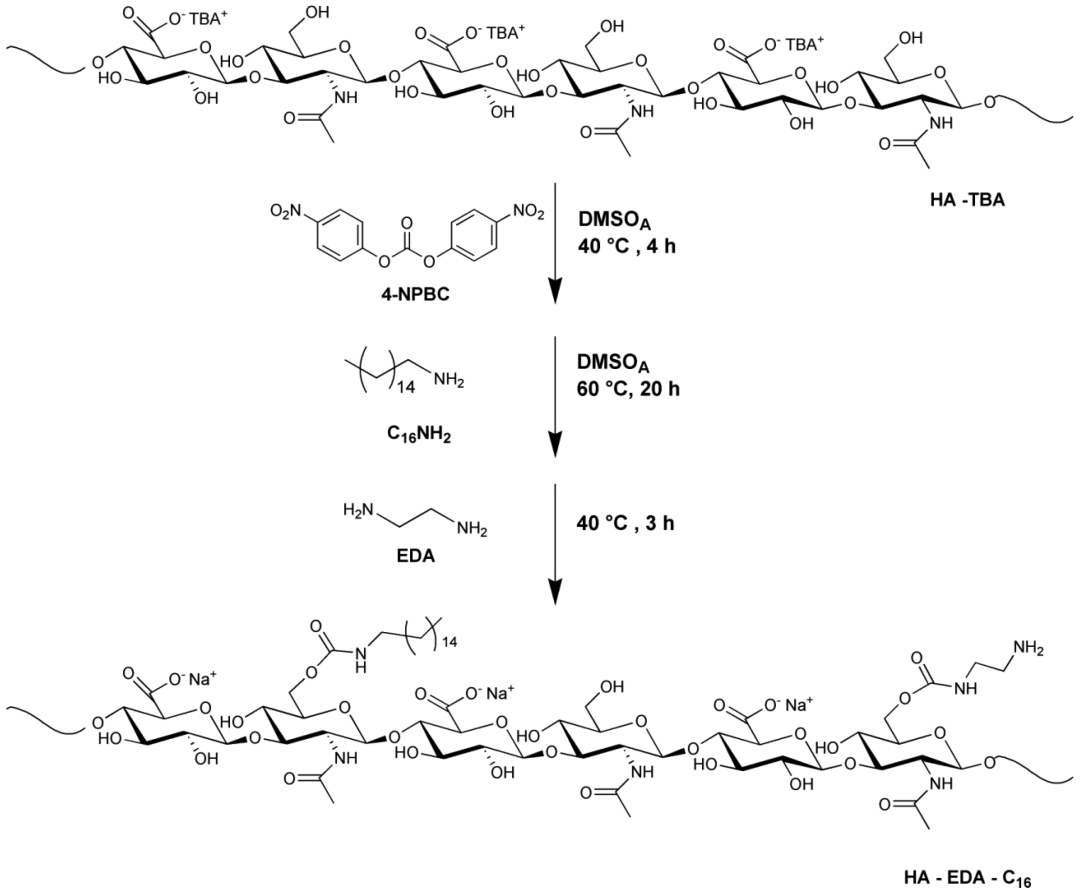

Table 1. Values of DD_{C16} mol %, DD_{EDA} mol %, DD_{PEG} mol %, DD_{CRN} mol %, Mw (kDa), and M_w/M_n of HA-EDA-C_{16}, HA-EDA-C_{16}−PEG, and HA-EDA-C_{16}−CRN

sample	DDC_{16} mol %	DD_{EDA} mol %	DD_{PEG} mol %	DD_{CRN} mol %	Mw (kDa)	M_w/M_n
HA-EDA-C_{16}	12.2 ± 0.03	48.4 ± 0.8			17.67	1.84
HA-EDA-C_{16}−PEG	12.2 ± 0.03	39.8 ± 1.7	6 ± 1.2		22.36	1.79
HA-EDA-C_{16}−CRN	12.2 ± 0.03	38.6 ± 0.9		7.2 ± 2.3	18.17	1.81

Statistical Analysis. All results were reported as means ± standard deviation (S.D.), and, when applicable, statistical analysis for significance was performed by means of Bonferroni's Multiple Comparison Test using GraphPad software. Values of $p < 0.05$ were considered statistically significant (∗), while a p-value < 0.01 (∗∗) and a p-value < 0.001 (∗∗∗) were considered as highly significant.

RESULTS AND DISCUSSION

Polymeric micelles were designed starting from the knowledge obtained in a previous work, in which a series of hexadecyl derivatives of hyaluronic acid was synthesized with a different degree of molar derivatization in C_{16} chains (7−15%).[40] In particular, HAC_{16} micelles (C_{16} molar amount of 12%) were able to entrap hydrophobic corticosteroids and to improve the transcorneal permeation profile by using *in vitro* and *ex vivo* models.[40] Here, the authors made a modification of the micellar external shell with potential corneal penetration enhancers such as PEG or L-carnitine to improve drug corneal permeation. For this reason, the synthesis of a new hyaluronic acid derivative named HA-EDA-C_{16} was reported. Ethylendiamine (EDA) was used to add primary amine groups available for functionalization with PEG or L-carnitine. HA-EDA-C_{16} derivative was synthesized following a chemical procedure consisting of the preliminary activation of primary hydroxyl groups of HA. This step was followed by nucleophilic substitution with hexadecylamine and then with ethylendiamine (Scheme 1). The molar amount of C_{16} chains linked to HA backbone (i.e., DD_{C16} mol %) was equal to 12.2% ± 0.03 (calculated by ^{1}H NMR, see Supplemental Figure III). The linked molar amount of EDA groups (i.e., DD_{EDA} mol %) was equal to 48.4% ± 0.8 (Table 1). The PEGylated derivative of HA-EDA-C_{16} was prepared through a Schiff-base chemistry that involved the terminal aldehyde group of PEG (Mw 2 kDa) and the −NH_2 of EDA groups. Reaction was conducted using a molar ratio between PEG-CHO and NH_2 groups of HA-EDA-C_{16} equal to 0.1 (Scheme 2).

DD_{PEG} mol % value was equal to 6% ± 1.2 (calculated by ^{1}H NMR, see Supplemental Figure IV). To confirm this value, TNBS assay was conducted to evaluate the reduction of free NH_2 groups on polymer derivative. The DD_{EDA} mol % value of HA-EDA-C_{16}−PEG decreased from 48.4% ± 0.8 (i.e., the

DOI: 10.1021/acs.molpharmaceut.8b00620
Mol. Pharmaceutics 2018, 15, 5031−5045

Scheme 2. Chemical Procedure for HA-EDA-C_{16} Derivatization with PEG-Aldehyde (PEG-CHO, Mw 2 kDa) To Obtain HA-EDA-C_{16}–PEG Derivative

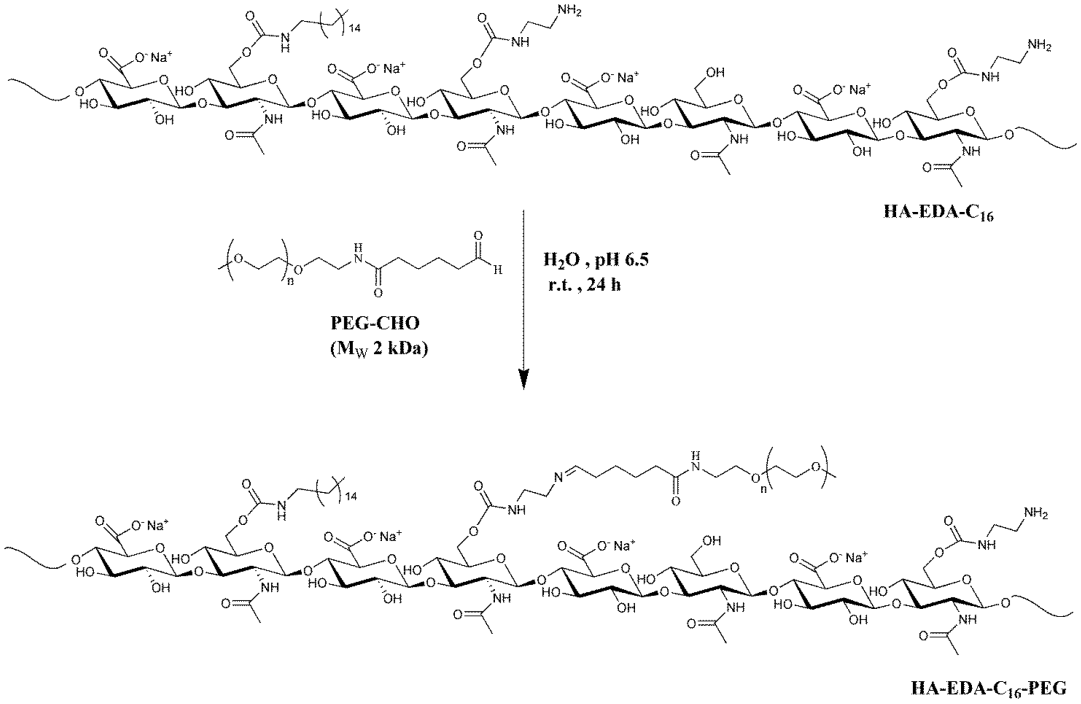

Scheme 3. Chemical Procedure for HA-EDA-C_{16} Derivatization with Activated L-Carnitine (CRN) To Obtain HA-EDA-C_{16}–CRN Derivative

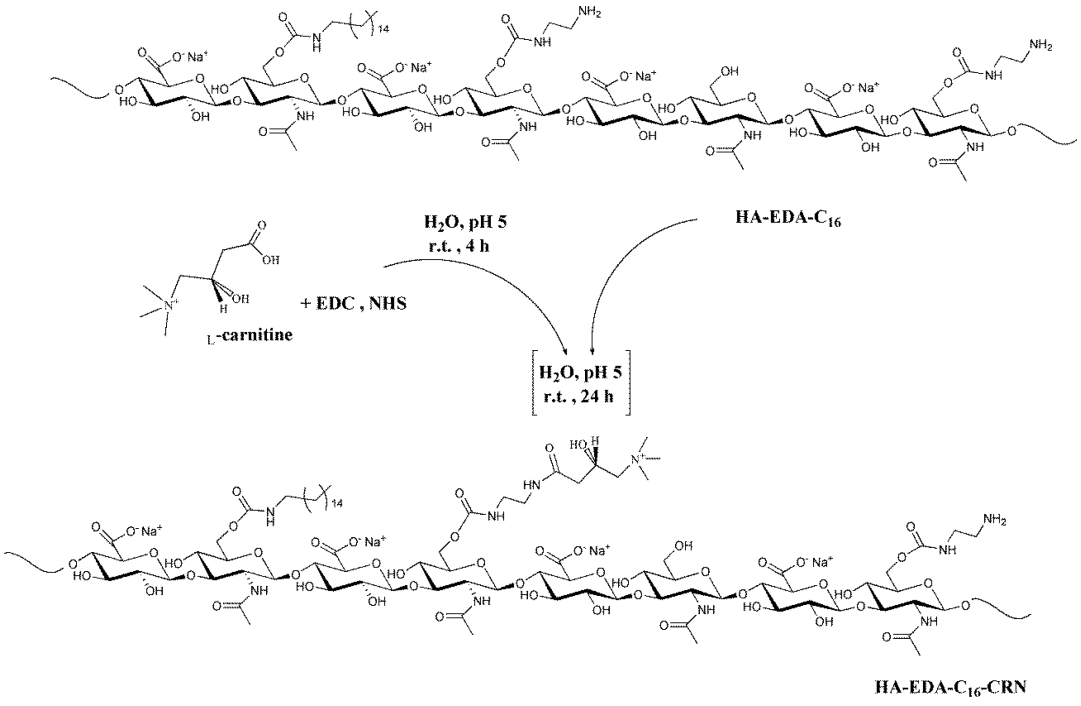

DD_{EDA} mol % value of starting HA-EDA-C_{16}) to 39.8% ± 1.7 (Table 1). A further confirmation of PEG derivatization was carried out with FT-IR analysis; HA-EDA-C_{16}–PEG spectrum was qualitatively compared to PEG and HA-EDA-C_{16} spectra (Supplemental Figure V). To synthesize HA-EDA-C_{16}–CRN derivative, the carboxyl group of L-carnitine was activated by EDC/NHS coupling method. Then activated L-carnitine was added in a HA-EDA-C_{16} water solution to obtain a molar ratio between CRN and EDA groups of HA-EDA-C_{16} equal to 0.1 (Scheme 3). HA-EDA-C_{16}–CRN derivative was characterized by a DD_{CRN} mol % value equal to 7.2% ± 2.3 (calculated by ^{1}H NMR, see Supplemental Figure VI). In addition, the reduction of free NH_2 groups from 48.4% ± 0.8 (i.e., the value of starting HA-EDA-C_{16}) to 38.6% ± 0.9 was evaluated by TNBS assay. HA-EDA-C_{16}, HA-EDA-C_{16}–PEG, and HA-EDA-C_{16}–CRN derivatives were characterized by SEC to evaluate their weight-

DOI: 10.1021/acs.molpharmaceut.8b00620
Mol. Pharmaceutics 2018, 15, 5031–5045

Table 2. CAC Values (mg/mL) in H_2O, DPBS, and HEPES Buffer of HAC_{16},[40] HA-EDA-C_{16}, HA-EDA-C_{16}−PEG, and HA-EDA-C_{16}−CRN Derivatives

sample	H_2O	DPBS	HEPES
HA-C_{16}	0.280 ± 0.010	0.170 ± 0.010	0.130 ± 0.020
HA-EDA-C_{16}	0.233 ± 0.014	0.119 ± 0.015	0.121 ± 0.010
HA-EDA-C_{16}−PEG	0.387 ± 0.017	0.138 ± 0.002	0.139 ± 0.014
HA-EDA-C_{16}−CRN	0.271 ± 0.005	0.140 ± 0.002	0.111 ± 0.001

Table 3. Values of Particle Size, PDI, and ζ-Potential of HA-EDA-C_{16}, HA-EDA-C_{16}−PEG, and HA-EDA-C_{16}−CRN Micelles in Bidistilled Water, DPBS, and HEPES Buffer

sample	dispersing medium	particle size (nm)	PDI	ζ-potential (mV)
HA-EDA-C_{16}	H_2O	231.5 ± 9.5	0.221	−37.6 ± 5.6
	DPBS	173.7 ± 7.4	0.293	−14.7 ± 2.8
	HEPES	145.8 ± 6.3	0.284	−10.2 ± 3.1
HA-EDA-C_{16}−PEG	H_2O	222.6 ± 2.9	0.198	−26.4 ± 4.9
	DPBS	157.7 ± 9.7	0.187	−10.3 ± 0.8
	HEPES	217.7 ± 1.2	0.204	−10.2 ± 1.1
HA-EDA-C_{16}−CRN	H_2O	226.8 ± 6.8	0.219	−20.1 ± 1.1
	DPBS	143.8 ± 4.3	0.176	−12.1 ± 0.9
	HEPES	211.5 ± 6.1	0.191	−10.6 ± 2.3

average molecular weight (Mw) (Table 1). HA-EDA-C_{16} derivative was characterized by CAC values (mg/mL) similar to those obtained for HAC_{16} derivative, as reported elsewhere.[40] This result confirmed that the presence of EDA groups not influenced the self-assembling property of HAC_{16} derivative (Table 2). Obtained data suggest that the presence of PEG (with a DD_{C16} mol % of 6% ± 1.2) or CRN (with a DD_{CRN} mol % of 7.2% ± 2.3) allowed to maintain the self-assembling property. In all investigated conditions, the CAC value for these derivatives was within the range of 0.1−0.4 mg/mL. In particular, lower values were obtained for micellar dispersion in DPBS and HEPES buffer. Reasonably, the ionic strength of these media allowed a strong aggregation, and then low CAC values were obtained.

HA-EDA-C_{16}, HA-EDA-C_{16}−PEG, and HA-EDA-C_{16}−CRN micelles were prepared by cosolvent evaporation method.[40−42] The positive influence of ionic strength on micellar aggregation was confirmed by the value of particle size in DPBS lower than that in bidistilled water. However, in HEPES buffer, this effect was less evident. The different saline composition of HEPES buffer (HEPES and NaCl) compared to DPBS (NaCl, KCl, Na_2HPO_4, KH_2PO_4) probably influenced polymeric aggregation in a different way (Table 3). In addition, HA-EDA-C_{16}−PEG and HA-EDA-C_{16}−CRN micelles in bidistilled water showed a value of ζ-potential lower than that of HA-EDA-C_{16} micelles, probably due to the exposition of PEG or L-carnitine in the external shell. All prepared micelles showed an interaction with mucin statistically higher ($p < 0.001$) than that observed for unmodified HA. The decoration of the micellar shell with PEG or L-carnitine has allowed to further increase the mucoadhesive characteristic compared to that shown by micelles HA-EDA-C_{16} ($p < 0.05$) (Figure 1). The formation of macro-aggregates occurred thanks to the mucoadhesive interaction between mucin and micelles; therefore, a decrease in transmittance values was observed.[43−45] In addition, obtained data suggest that a time-independent mucoadhesion process occurred for each sample.

Imatinib free base (I) was chosen as a TKI molecule able to potentially inhibit ocular neovascularization processes. Micelles of HA-EDA-C_{16}, HA-EDA-C_{16}−PEG, or HA-EDA-C_{16}−CRN

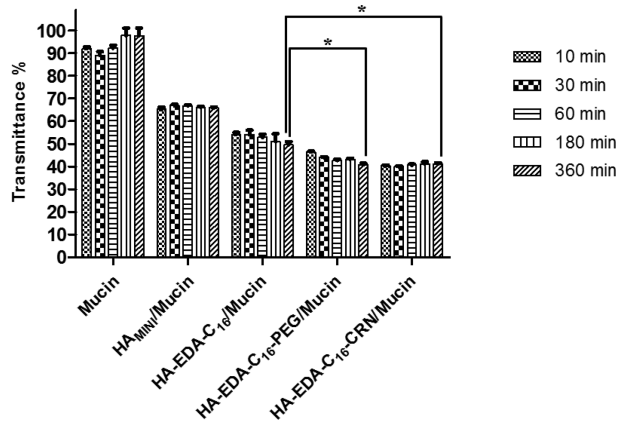

Figure 1. Transmittance % values of mixture of mucin with micelles (HA-EDA-C_{16}, HA-EDA-C_{16}−PEG, or HA-EDA-C_{16}−CRN) or starting HA_{MINI} as a function of time.

were able to entrap this drug and resulting drug-loaded micelles showed a particle size lower than the empty micelles (Table 4). Probably, a stronger hydrophobic interaction between hexadecyl chains and lipophilic drug molecules (Log P = 3) occurred to promote the formation of smaller micelles (<200 nm). Imatinib release profile from HA-EDA-C_{16}/I, HA-EDA-C_{16}−PEG/I, and HA-EDA-C_{16}−CRN/I micelles was studied in DPBS. The diffusion of free drug from solution and suspension was analyzed in the same conditions (Figure 2). To prepare imatinib solution, the drug was dissolved in methanol and then diluted in DPBS at final concentration of 0.025 mg/mL (S_{MAX} imatinib < 0.0146 mg/mL).[13,46] Drug molecules diffused completely within 48 h. Organic solvent (MeOH) was not necessary for the preparation of other samples. After 48 h, a drug amount of 16.38% ± 0.11 was released by using drug suspension. An amount of 75.20% ± 2.62, 82.97% ± 1.53, 71.49% ± 1.73 was released by using HA-EDA-C_{16}, HA-EDA-C_{16}−PEG, and HA-EDA-C_{16}−CRN micelles, respectively ($p < 0.05$). Therefore, investigated micelles are able to rapidly release a large amount of imatinib, with an initial therapeutic dose followed by a drug sustained release. Therefore, release profiles obtained could be beneficial in the ocular therapy.[47]

DOI: 10.1021/acs.molpharmaceut.8b00620
Mol. Pharmaceutics 2018, 15, 5031−5045

Table 4. Values of Drug Loading (DL%), Particle Size, PDI, and ζ-Potential of HA-EDA-C_{16}, HA-EDA-C_{16}−PEG, and HA-EDA-C_{16}−CRN Micelles in Bidistilled Water, DPBS, and HEPES Buffer

sample	DL % (w/w)	dispersing medium	particle size	PDI	ζ-potential
HA-EDA-C_{16}/I	13.1 ± 0.5	H_2O	193.3 ± 8.2	0.282	−33.3 ± 3.7
		DPBS	164.1 ± 4.9	0.230	−19.5 ± 2.9
		HEPES	143.7 ± 7.2	0.280	−11.8 ± 1.7
HA-EDA-C_{16}−PEG/I	12.6 ± 0.8	H_2O	180.4 ± 11	0.208	−22.6 ± 4.3
		DPBS	191.6 ± 8.4	0.184	−18.1 ± 3.8
		HEPES	135.5 ± 11	0.202	−10.9 ± 0.5
HA-EDA-C_{16}−CRN/I	11.2 ± 0.4	H_2O	165.7 ± 4.9	0.176	−23.8 ± 4.3
		DPBS	143 ± 7.3	0.201	−16.4 ± 1.7
		HEPES	128.9 ± 4.7	0.196	−12.4 ± 1.8

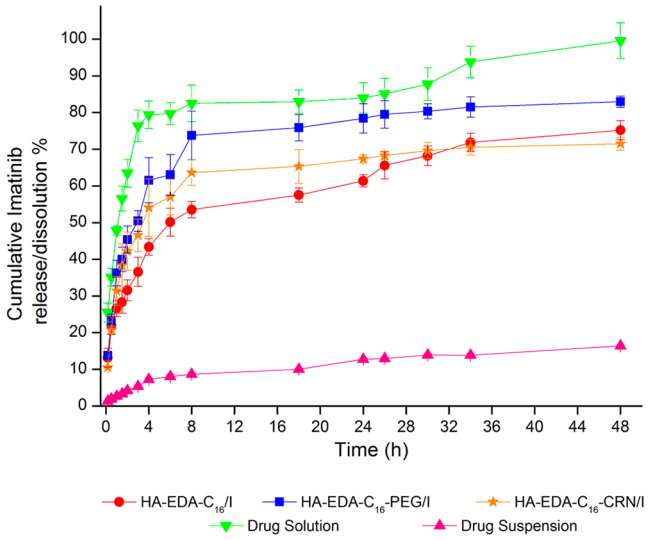

Figure 2. Cumulative imatinib release/dissolution % from free drug solution (▼ green), free drug suspension (▲ pink), HA-EDA-C_{16} micelles (● red), HA-EDA-C_{16}−PEG micelles (■ blue), HA-EDA-C_{16}−CRN micelles (∗ orange) until 48 h. Data represent means ± SD (n = 3).

HA-EDA-C_{16}, HA-EDA-C_{16}−PEG, and HA-EDA-C_{16}−CRN micelles showed appropriate size, mucoadhesive properties, optimal drug loading capacity, and ability to sustain imatinib release. By taking into account these advantageous characteristics, all micellar systems were sterilized and their cytocompatibility was evaluated on human corneal epithelial cells (HCEpiC). The selected sterilization process allowed researchers to maintain the properties of micelles unaltered in terms of entrapped quantity of drug and particle size (Supplemental Table 2). After the incubation of cells with different micelle concentrations, HCEpiC viability was maintained and values greater than 70% compared to untreated cell control were obtained (ISO 10993−5) (Supplemental Figure VII). In addition, the stability of all micelles when dispersed in HCEpiC culture medium was confirmed until 7 days at 37 °C (Supplemental Figure VIII). *In vitro* and *ex vivo* permeation experiments were performed to evaluate the ability of micellar systems to interact with corneal epithelial cells or with corneal structure. A transwell system was used for *in vitro* permeation experiments through a HCEpiC monolayer. HA-EDA-C_{16}−PEG-AlexaFluor$_{488}$ and HA-EDA-C_{16}−CRN-AlexaFluor$_{488}$ micelles showed a favorable permeation profile compared to that obtained for HA-EDA-C_{16}−AlexaFluor$_{488}$ micelles (p < 0.001) (Figure 3A). Probably, micellar shell decoration with PEG or CRN improved the

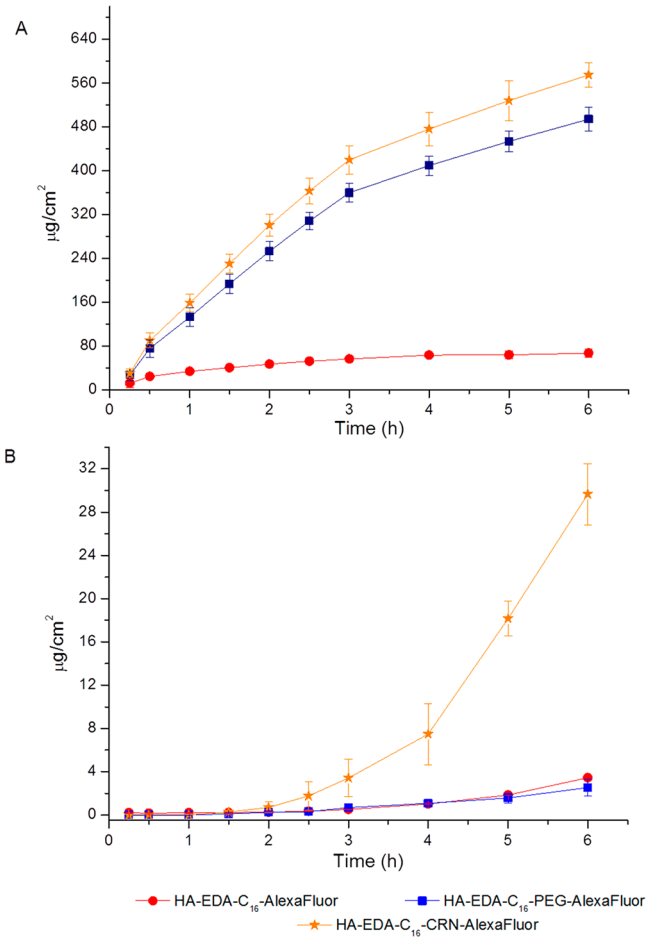

Figure 3. (A) *In vitro* and (B) *ex vivo* transcorneal permeation profiles of HA-EDA-C_{16}−AlexaFluor$_{488}$, HA-EDA-C_{16}−PEG-AlexaFluor$_{488}$, and HA-EDA-C_{16}−CRN-AlexaFluor$_{488}$ micelles ($\mu g/cm^2$ of permeated micelles as a function of incubation time).

interaction between amphiphilic copolymers and cell monolayer. In addition, a greater value was obtained for HA-EDA-C_{16}−CRN-AlexaFluor$_{488}$ micelles compared to HA-EDA-C_{16}−PEG-AlexaFluor$_{488}$ micelles at the end of experiment (p < 0.01). In the *ex vivo* experiment, HA-EDA-C_{16}−CRN-AlexaFluor$_{488}$ micelles showed a strong ability to permeate the corneal barrier. A weaker interaction between these micelles and corneal stroma probably occurred until 6 h, compared to PEGylate and free hyaluronic acid micelles. In fact, HA-EDA-C_{16}−PEG-AlexaFluor$_{488}$ and HA-EDA-C_{16}−AlexaFluor$_{488}$ micelles showed a retarded permeation profile (Figure 3B). For these samples, the different hydrophilic/

DOI: 10.1021/acs.molpharmaceut.8b00620
Mol. Pharmaceutics 2018, 15, 5031−5045

hydrophobic balance of amphiphilic polymer forming micelles probably causes an increased interaction with corneal barrier. In addition, the mucoadhesive properties of all micelles should be also considered. The stronger mucoadhesive behavior of PEGylated- and L-carnitine-micelles compared to free hyaluronic acid micelles could prolong the contact time between nanocarriers and corneal epithelium and, consequently, promote the accumulation and permeation of micelles. Therefore, both mucoadhesion and ability of micelles to interact with corneal structure are two aspects that potentially could increase the drug permeation through corneal barrier.

With the aim to confirm the ability of these micelles to improve imatinib transcorneal permeation, all drug-loaded micellar dispersions were also tested using *in vitro* and *ex vivo* models. *In vitro* experiments confirmed the ability of HA-EDA-C_{16}–PEG and HA-EDA-C_{16}–CRN micelles to improve drug permeation if compared with permeation profile of imatinib solution ($p < 0.01$ and $p < 0.001$, respectively) (Figure 4A). *Ex vivo* experiments showed that all micelles improved imatinib permeation through corneal barrier after a lag time of 2 h (Figure 4B). HA-EDA-C_{16}–PEG and HA-EDA-C_{16}–CRN micelles allowed an equal drug permeation until 6 h.

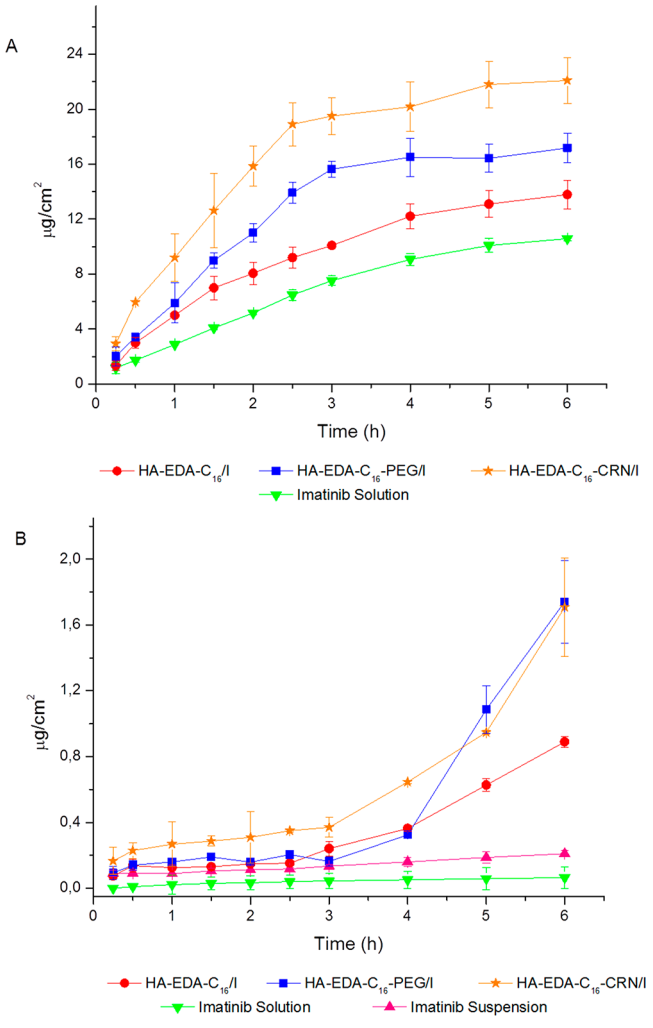

Figure 4. (A) *In vitro* and (B) *ex vivo* transcorneal permeation profiles of imatinib using drug solution, drug suspension, HA-EDA-C_{16}/I, HA-EDA-C_{16}–PEG/I, and HA-EDA-C_{16}–CRN/I micelles ($\mu g/cm^2$ of permeated drug as a function of incubation time).

Compared with free hyaluronic acid micelles, a higher permeation profile of imatinib was observed when drug was delivered from HA-EDA-C_{16}–PEG micelles ($p < 0.01$) or HA-EDA-C_{16}–CRN micelles ($p < 0.01$). This result allows researchers to suppose that micellar shell decoration with PEG or CRN increased the drug stromal diffusion and then transcorneal permeation.

In addition, although methanol traces in imatinib solution could promote transcorneal permeation, the high hydrophobicity of imatinib (Log P = 3) probably limited strongly the interaction with the amphiphilic barrier. In the case of imatinib suspension, drug molecules could precipitate on corneal surface and this could hinder drug transcorneal permeation (Figure 4B).

At the end of each *ex vivo* experiment, the amount of drug retained into the cornea was evaluated and expressed as μg of drug per cm^2 of tissue (Table 5). HA-EDA-C_{16} micelles allowed to increase imatinib corneal retention of 11.51- and 9.46-times compared to drug solution and drug suspension, respectively. HA-EDA-C_{16}–CRN micelles allowed an increase of 13.15 and 10.81, respectively, while imatinib corneal retention was increased of 5.17- and 4.25-times when using HA-EDA-C_{16}–PEG micelles compared to drug solution and suspension.

The PEGylation of micelles probably allowed to increase their interaction with stromal compartment; therefore, imatinib retention was reduced. For this reason, the role of HA-EDA-C_{16}–PEG micelles as penetration enhancers was less evident compared to the HA-EDA-C_{16} and HA-EDA-C_{16}–CRN micelles. All data obtained from these permeation studies were used to calculate imatinib fluxes (J_s) and imatinib permeability coefficients (K_p) through the HCEpiC monolayer or bovine cornea[35,40,48] (Table 6). The flux (J_s) and the permeability coefficient (K_p) were determined by using the eqs 1 and 2, respectively:

$$J_s = Q/(A \times t)\ (\mu g\ cm^{-2}\ h^{-1}) \quad (1)$$

$$K_p = J_s/C_D\ (cm/h) \quad (2)$$

In these equations, Q was the amount of drug (μg) that crossed the monolayer/cornea and that arrived into the acceptor chamber, A was the effective area available for permeation (0.33 cm^2 for *in vitro* study, 1.1304 cm^2 for *ex vivo* study), t was the exposure time (h), and C_D was the drug concentration loaded into the donor chamber ($\mu g/cm^3$).

For the *in vitro* study, the K_p value of imatinib solution was greater than that obtained with HA-EDA-C_{16} micelles ($p < 0.01$) and it was equal to that obtained by using HA-EDA-C_{16}–PEG micelles. Probably, the presence of residual methanol in imatinib solution (less than 1% v/v) promoted drug permeation.[49] HA-EDA-C_{16}–CRN micelles were capable to improve the drug permeation in the *in vitro* model. An increase in K_p value of 1.46-times was obtained by using these micelles compared to imatinib solution ($p < 0.001$). In addition, micelles decorated with L-carnitine were capable to increase *in vitro* imatinib permeation compared to HA-EDA-C_{16} ($p < 0.001$) and HA-EDA-C_{16}–PEG micelles ($p < 0.05$). Obtained K_p value from *ex vivo* experiment confirmed the potential role of micelles to improve the transcorneal permeation and penetration of imatinib. HA-EDA-C_{16}, HA-EDA-C_{16}–PEG, and HA-EDA-C_{16}–CRN micelles increased imatinib K_p value of 10.5-, 20.5-, and 16.5-times compared to drug suspension ($p < 0.001$ for all samples). In addition, a

DOI: 10.1021/acs.molpharmaceut.8b00620
Mol. Pharmaceutics 2018, 15, 5031–5045

Table 5. Imatinib Amount ($\mu g/cm^2$) Retained into Cornea at the End of *ex Vivo* Transcorneal Permeation Study

drug solution	drug suspension	HA-EDA-C_{16} micelles	HA-EDA-C_{16}–PEG micelles	HA-EDA-C_{16}–CRN micelles
1.29 ± 0.27	1.57 ± 0.21	14.86 ± 0.88	6.67 ± 1.2	16.97 ± 1.07

Table 6. Values of Flux (J_s, $\mu g/cm^2\ h^{-1}$) and Permeability Coefficient (K_p, cm/h) of Imatinib Using Free Drug Solution, Free Drug Suspension, and Drug-Loaded Micelles through HCEpiC Monolayer (*in Vitro* Permeation Study, A) and Bovine Cornea (*ex Vivo* Permeation Study, B)

A	J_s	K_p
drug solution	2.330 ± 0.171	0.09321 ± 0.00832
HA-EDA-C_{16}/I	3.071 ± 0.164	0.06143 ± 0.00351
HA-EDA-C_{16}–PEG/I	5.042 ± 0.104	0.10086 ± 0.00208
HA-EDA-C_{16}–CRN/I	6.802 ± 0.139	0.13604 ± 0.00173
B	**J_s**	**K_p**
drug solution	0.007 ± 0.001	0.00028 ± 0.00003
drug suspension	0.020 ± 0.004	0.00004 ± 0.00002
HA-EDA-C_{16}/I	0.208 ± 0.011	0.00042 ± 0.00002
HA-EDA-C_{16}–PEG/I	0.406 ± 0.009	0.00082 ± 0.00003
HA-EDA-C_{16}–CRN/I	0.331 ± 0.005	0.00066 ± 0.00004

statistically significant increase was evaluated when all micelles were compared to imatinib solution ($p < 0.01$ for HA-EDA-C_{16} micelles; $p < 0.001$ for HA-EDA-C_{16}–PEG and HA-EDA-C_{16}–CRN micelles). Therefore, the results obtained confirm that the prepared micelles could allow the release of imatinib free base in the eye, modulating also its transcorneal permeation over time.

By taking into account the advantages of these nanocarriers, further studies *in vitro* were conducted to investigate the imatinib effect on neovascularization process. It is known that close cell–cell connections of sprouting endothelial cells, pericytes or their progenitor mesenchymal cells allow the formation of functional blood vessels.[15] To evaluate the endothelial cell interactions during vessel formation, the sprouting assay can be used as an *in vitro* model. For this reason, to evaluate if imatinib was able to act on vessel-associated tissue produced by endothelial cells, the tube formation assay was performed on HUVEC in ECM matrix. ECM matrix was used with endothelial cells thanks to the presence of several pro-angiogenic growth factors; during angiogenesis, produced ECM seemed to be essential to create a structure along which endothelial cells establish vascular complexes. For the first time, HUVEC viability was confirmed by using imatinib solution with a concentration less than 25 $\mu g/mL$ (equal to 50.65 pM). In addition, the low presence of methanol (less than 1% v/v) was safe for cells under these experimental conditions (Supplemental Figure IX). In the concentration range of 5–25 $\mu g/mL$, imatinib solution was tested for the *in vitro* tube formation assay (see Experimental

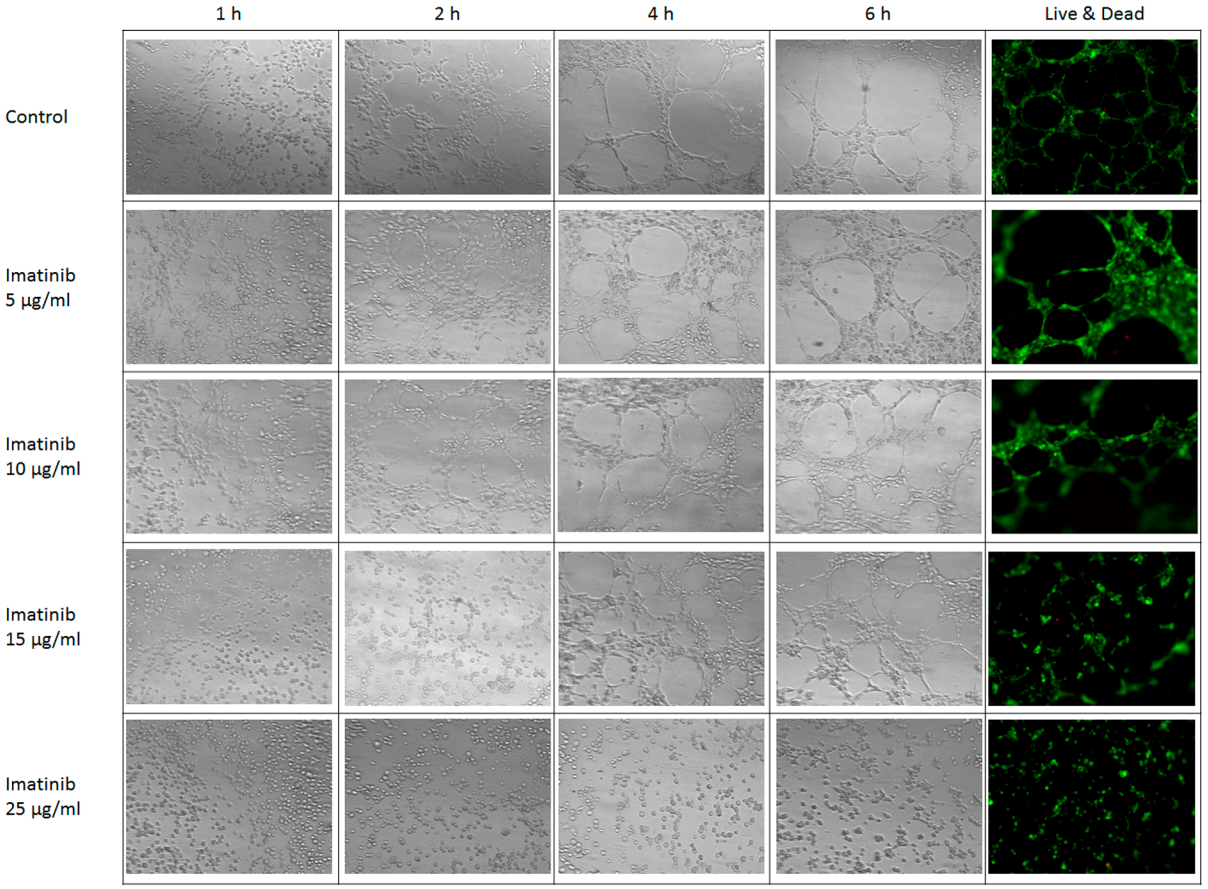

Figure 5. Image analysis of endothelial cell tube formation on EHS matrix. Cell control and cell treated with imatinib solution (5–25 $\mu g/mL$) until 6 h. Right Column: Live&Dead assay conducted at the end of the experiment.

DOI: 10.1021/acs.molpharmaceut.8b00620
Mol. Pharmaceutics 2018, 15, 5031–5045

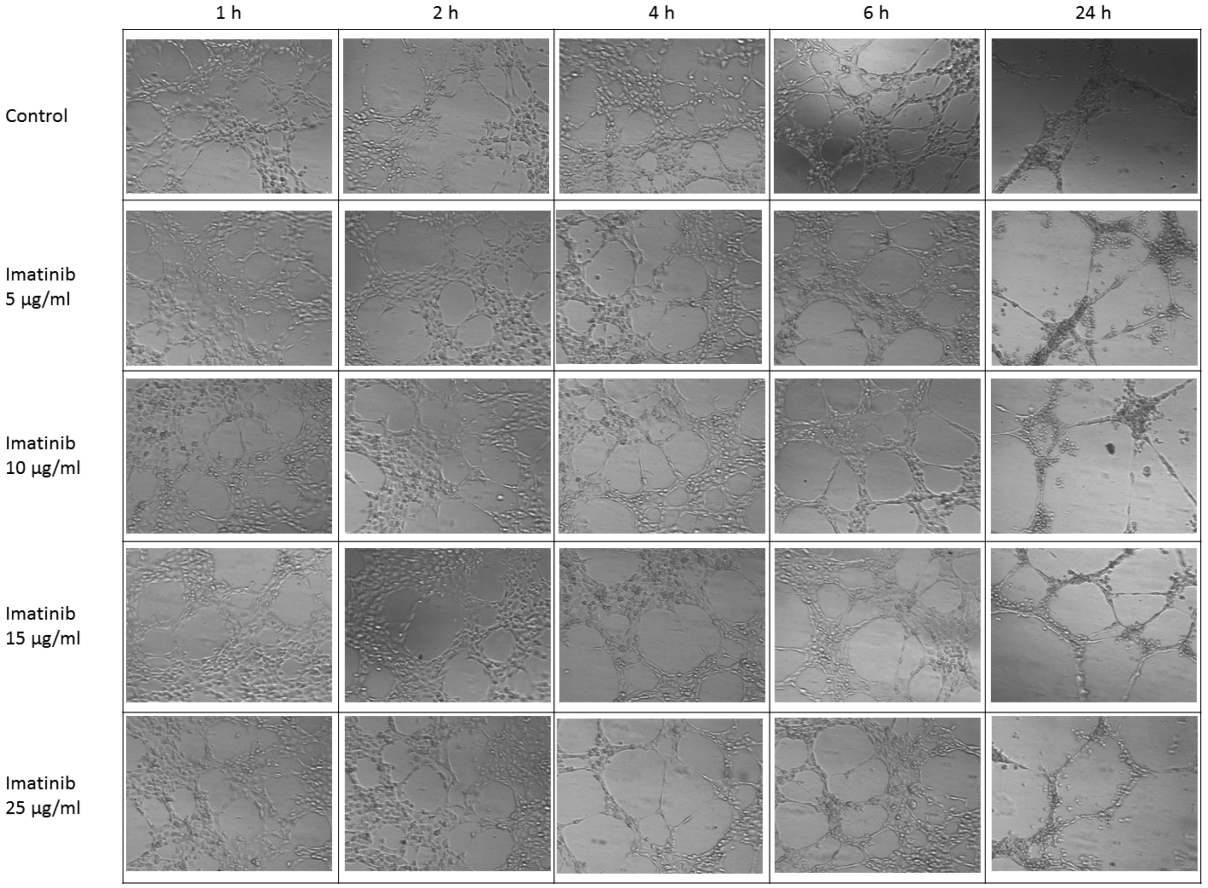

Figure 6. Structural regression of endothelial cell tube on EHS matrix. Cell control and cell treated with imatinib solution (5−25 μg/mL) until 24 h.

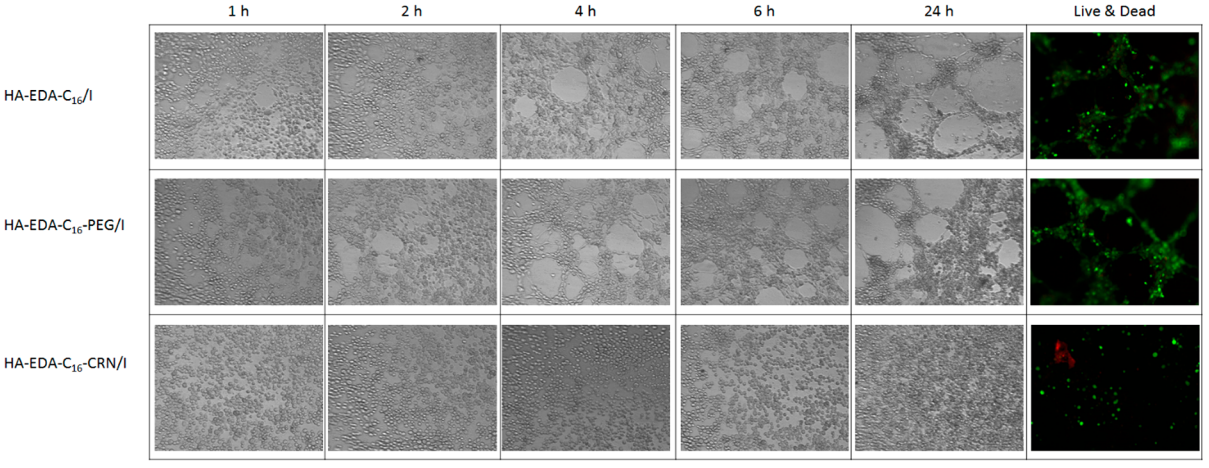

Figure 7. Image analysis of endothelial cell tube formation on EHS matrix. Cell treated with HA-EDA-C_{16}/I, HA-EDA-C_{16}−PEG/I, and HA-EDA-C_{16}−CRN/I micelles (imatinib concentration equal to 40 μg/mL) until 24 h. Right Column: Live&Dead assay conducted at the end of experiment.

Section). After 6 h of treatment, a limited HUVEC sprouting process was evident using an imatinib solution of 15 μg/mL. On the contrary, imatinib at 25 μg/mL was able to inhibit the formation of endothelial cell tubes (Figure 5). Also the ability of imatinib to cause the disruption of endothelial cell tube structures was confirmed *in vitro*. In particular, this effect was more evident using imatinib solution at 25 μg/mL (Figure 6). To evaluate imatinib efficacy when released from micelles, a similar study was performed by using HA-EDA-C_{16}/I, HA-EDA-C_{16}−PEG/I, and HA-EDA-C_{16}−CRN/I micelles. Employed imatinib concentration was equal to 40 μg/mL, considering that micelles were capable to release drug molecules in a modulated way during experimental time (48 h) (see Figure 2). Chosen experimental conditions (in terms of concentration of empty and imatinib-loaded micelles) allowed to maintain HUVEC viability until 24 h (Supplemental Figure X). Therefore, imatinib-loaded micelles were tested for the *in vitro* cell tube formation assay. When micelles were loaded within endothelial cells on the top of EHS matrix, the inhibitory effect of imatinib was confirmed until 24 h. In

DOI: 10.1021/acs.molpharmaceut.8b00620
Mol. Pharmaceutics 2018, 15, 5031−5045

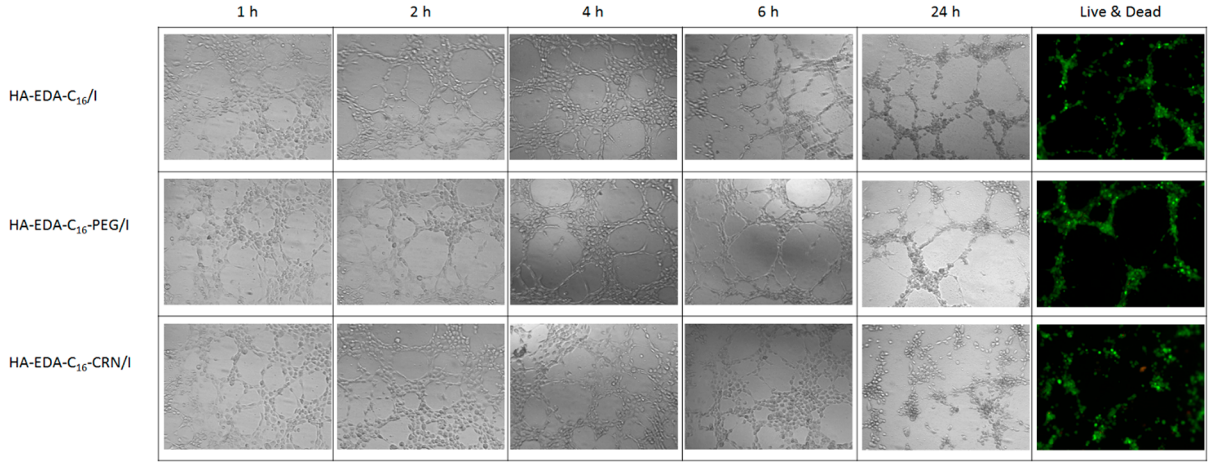

Figure 8. Structural regression of endothelial cell tube on EHS matrix after HA-EDA-C_{16}/I, HA-EDA-C_{16}–PEG/I, and HA-EDA-C_{16}–CRN/I micelles treatment (imatinib concentration equal to 40 μg/mL) until 24 h. Right Column: Live&Dead assay conducted at the end of the experiment.

particular, a limited and random inhibition of HUVEC sprouting was observed when HA-EDA-C_{16}/I and HA-EDA-C_{16}–PEG/I micelles were used. In the case of HA-EDA-C_{16}–CRN/I micelles, a stronger inhibitory effect was assessed after 24 h of treatment; cells appeared isolated from each other (Figure 7). Imatinib was able also to reduce preformed cell tubular structures when administered within the micelles (Figure 8). The micrograph of the Live&Dead test allowed to evaluate a visible reduction of cellular interactions, probably in terms of both number and entity. Furthermore, a higher inhibitory effect appeared with HA-EDA-C_{16}–CRN/I micelles compared to HA-EDA-C_{16}/I and HA-EDA-C_{16}–PEG/I micelles. Probably, the presence of L-carnitine improved the interaction with endothelial cells and consequently the efficacy of imatinib.

Obtained data suggest the potential of imatinib in the treatment of retinopathies. VEGF and PDGF are the most significant known growth factors implicated in the choroidal neovascularization process. Therefore, a combined inhibition of VEGF/PDGF receptors by imatinib could allow a more specific and especially improved management of retinopathies.

In fact, the additional inhibition of PDGF (compared to the alone inhibition of VEGF) could reduce the disordered proliferation of cells and the ECM that accompany neovascularization with a consequent improvement in the efficacy of the therapeutic treatment.

CONCLUSION

In this study, the off-label use of imatinib to treat neoangiogenesis in an experimental *in vitro* model was assessed. A preliminary characterization confirmed the efficacy of imatinib, at different aqueous concentration, to inhibit the endothelial cell sprouting and to reduce potentially the formation of functional vessels. In addition, compared to the use of free drug or no drug treatment, imatinib significantly inhibited endothelial cell tube formation as well as promoted cell tube disruption on EHS matrix when released from polymeric micelles prepared using appropriate hyaluronic acid derivatives. In particular, micelles were prepared by using hyaluronic acid (HA) derivatives containing chains of ethylenediamine (EDA), hexadecyl (C_{16}), polyethylene glycol (PEG), or L-carnitine (CRN). Resulting samples, named as HA-EDA-C_{16}, HA-EDA-C_{16}–PEG, and HA-EDA-C_{16}–CRN micelles, allowed researchers to load imatinib and to obtain a biological effect maintaining cell viability and above all avoiding the use of methanol. Another important outcome was that these polymeric systems could potentially be administered non-invasively, that is, by topical ocular instillation. Indeed, these systems showed appropriate particle size in different media (lower than 300 nm) and mucoadhesive properties. Above all, micelles were able to interact with corneal barrier and to promote the transcorneal permeation and penetration of imatinib. Obtained results suggest that prepared micelles could represent optimal candidates for off-label use of imatinib in the potential treatment of retinopathies.

ASSOCIATED CONTENT

Supporting Information

The Supporting Information is available free of charge on the ACS Publications website at DOI: 10.1021/acs.molpharmaceut.8b00620.

Stability of fluorescent labeled, empty, and drug-loaded micelles; ^{1}H NMR spectra of HA-EDA-C_{16}, HA-EDA-C_{16}–PEG, and HA-EDA-C_{16}–CRN; FT-IR spectra of PEG-aldehyde, HA-EDA-C_{16}, and HA-EDA-C_{16}–PEG; *in vitro* HCEpiC and HUVEC viability data (PDF)

AUTHOR INFORMATION

Corresponding Author

*E-mail giovanna.pitarresi@unipa.it. Phone: +3909123891954. Fax +390916100627.

ORCID

Giovanna Pitarresi: 0000-0002-0815-9142

Present Address

§G.D.P., Consiglio Nazionale delle Ricerche – Istituto di Biofisica, Via Ugo La Malfa 153, 90146, Palermo, Italy.

Notes

The authors declare no competing financial interest.

ACKNOWLEDGMENTS

This work has been funded by MIUR by means of the National Program PON R&C 2007-2013, "Piattaforma scientifico-tecnologica mirata allo sviluppo di nuovi approcci terapeutici

DOI: 10.1021/acs.molpharmaceut.8b00620
Mol. Pharmaceutics 2018, 15, 5031–5045

nel trattamento delle principali patologie degenerative della retina, REACT (REtinopathies Advanced Care Therapies)" (PON01_01434). The authors thank Dr. Roberto Puleio of Istituto Zooprofilattico della Sicilia "A. Mirri", Palermo, Italy, and Dr. Gaspare Orlando of the local Departmentof Veterinary Prevention (ASP-Palermo, Italy) for providing animal tissues.

■ ABBREVIATIONS

4-NPBC, bis(4-nitrophenyl)carbonate; $C_{16}NH_2$, hexadecylamine; CRN, L-carnitine; $DMSO_A$, anhydrous dimethyl sulfoxide; EDA, ethylenediamine; EDC, N-(3-(dimethylamino)propyl)-N′-ethylcarbodiimide hydrochloride; EtOH, ethanol; HA, hyaluronic acid; HA-TBA, tetrabutylammonium salt of HA; HCEpiC, human corneal epithelial cells; HEPES, 4-(2-hydroxyethyl)piperazine-1-ethanesulfonic acid; HUVEC, human umbilical vein endothelial cells; I, imatinib free base; MeOH, methanol; NHS, *N*-hydroxysuccinimide; NRP1, neuropilin 1; OCTN, organic cation transporter system; PDGF-B, platelet derived growth factor-B; PDGFR-*β*, platelet derived growth factor receptor-*β*; PDI, polydispersity index; PEG, polyethylene glycol; Ph+CML, Philadelphia positive chronic myeloid leukemia; PLGA, poly(D,L-lactide-*co*-glycolide); TKI, tyrosine kinase inhibitor; TNBS, 2,4,6-trinitrobenzenesulfonic acid; VEGF, vascular endothelial growth factor

■ REFERENCES

(1) Hellström, A.; Smith, L. E. H. H; Dammann, O. Retinopathy of prematurity. *Lancet* **2013**, *382*, 1445−1457.
(2) Bhutto, I.; Lutty, G. Understanding age-related macular degeneration (AMD): Relationships between the photoreceptor/retinal pigment epithelium/Bruch's membrane/choriocapillaris complex. *Mol. Aspects Med.* **2012**, *33*, 295−317.
(3) Kaur, I. P.; Kakkar, S. Nanotherapy for posterior eye diseases. *J. Controlled Release* **2014**, *193*, 100−112.
(4) Ahmad, I.; Balasubramanian, S.; Del Debbio, C. B.; Parameswaran, S.; Katz, A. R.; Toris, C.; Fariss, R. N. Regulation of ocular angiogenesis by Notch signaling: Implications in neovascular age-related macular degeneration. *Invest. Ophthalmol. Visual Sci.* **2011**, *52*, 2868−2878.
(5) Kim, L. A.; D'Amore, P. A. A brief history of anti-VEGF for the treatment of ocular angiogenesis. *Am. J. Pathol.* **2012**, *181*, 376−379.
(6) Bradley, J.; Ju, M.; Robinson, G. S. Combination therapy for the treatment of ocular neovascularization. *Angiogenesis* **2007**, *10*, 141−148.
(7) Bergers, G.; Song, S.; Meyer-Morse, N.; Bergsland, E.; Hanahan, D. Benefits of targeting both pericytes and endothelial cells in the tumor vasculature with kinase inhibitors. *J. Clin. Invest.* **2003**, *111*, 1287−1295.
(8) Kang, S.; Roh, Y. J.; Kim, I. B. Antiangiogenic effects of tivozanib, an oral VEGF receptor tyrosine kinase inhibitor, on experimental choroidal neovascularization in mice. *Exp. Eye Res.* **2013**, *112*, 125−133.
(9) Wu, P.; Nielsen, T. E.; Clausen, M. H. Small-molecule kinase inhibitors: an analysis of FDA-approved drugs. *Drug Discovery Today* **2016**, *21*, 5−10.
(10) Raimondi, C.; Fantin, A.; Lampropoulou, A.; Denti, L.; Chikh, A.; Ruhrberg, C. Imatinib inhibits VEGF-independent angiogenesis by targeting neuropilin 1-dependent ABL1 activation in endothelial cells. *J. Exp. Med.* **2014**, *211*, 1167−83.
(11) Roskoski, R. A historical overview of protein kinases and their targeted small molecule inhibitors. *Pharmacol. Res.* **2015**, *100*, 1−23.
(12) Buchdunger, E.; O'Reilley, T.; Wood, J. Pharmacology of imatinib (STI571). *Eur. J. Cancer* **2002**, *38*, S28−S36.
(13) Gupta, B.; Poudel, B. K.; Tran, T. H.; Pradhan, R.; Cho, H. J.; Jeong, J. H.; Shin, B. S.; Choi, H. G.; Yong, C. S.; Kim, J. O. Modulation of Pharmacokinetic and Cytotoxicity Profile of Imatinib Base by Employing Optimized Nanostructured Lipid Carriers. *Pharm. Res.* **2015**, *32*, 2912−2927.
(14) Ramazani, F.; Chen, W.; Van Nostrum, C. F.; Storm, G.; Kiessling, F.; Lammers, T.; Hennink, W. E.; Kok, R. J. Formulation and characterization of microspheres loaded with imatinib for sustained delivery. *Int. J. Pharm.* **2015**, *482*, 123−130.
(15) Giddabasappa, A.; Lalwani, K.; Norberg, R.; Gukasyan, H. J.; Paterson, D.; Schachar, R. A.; Rittenhouse, K.; Klamerus, K.; Mosyak, L.; Eswaraka, J. Axitinib inhibits retinal and choroidal neovascularization in in vitro and in vivo models. *Exp. Eye Res.* **2016**, *145*, 373−379.
(16) Zhang, N.; Wardwell, P. R.; Bader, R. A. Polysaccharide-based micelles for drug delivery. *Pharmaceutics* **2013**, *5*, 329−352.
(17) Agnello, S.; Bongiovì, F.; Fiorica, C.; Pitarresi, G.; Palumbo, F. S.; Di Bella, M. A.; Giammona, G. Microfluidic Fabrication of Physically Assembled Nanogels and Micrometric Fibers by Using a Hyaluronic Acid Derivative. *Macromol. Mater. Eng.* **2017**, *302*, 1700265.
(18) Palumbo, F. S.; Fiorica, C.; Di Stefano, M.; Pitarresi, G.; Gulino, A.; Agnello, S.; Giammona, G. In situ forming hydrogels of hyaluronic acid and inulin derivatives for cartilage regeneration. *Carbohydr. Polym.* **2015**, *122*, 408−416.
(19) Palumbo, F. S.; Agnello, S.; Fiorica, C.; Pitarresi, G.; Puleio, R.; Loria, G. R.; Giammona, G. Spray dried hyaluronic acid microparticles for adhesion controlled aggregation and potential stimulation of stem cells. *Int. J. Pharm.* **2017**, *519*, 332−342.
(20) Palumbo, F. S.; Pitarresi, G.; Mandracchia, D.; Tripodo, G.; Giammona, G. New graft copolymers of hyaluronic acid and polylactic acid: Synthesis and characterization. *Carbohydr. Polym.* **2006**, *66*, 379−385.
(21) Fiorica, C.; Palumbo, F. S.; Pitarresi, G.; Bongiovì, F.; Giammona, G. Hyaluronic acid and beta cyclodextrins films for the release of corneal epithelial cells and dexamethasone. *Carbohydr. Polym.* **2017**, *166*, 281−290.
(22) Palumbo, F. S.; Pitarresi, G.; Fiorica, C.; Matricardi, P.; Albanese, A.; Giammona, G. In situ forming hydrogels of new amino hyaluronic acid/benzoyl-cysteine derivatives as potential scaffolds for cartilage regeneration. *Soft Matter* **2012**, *8*, 4918.
(23) Palumbo, F. S.; Agnello, S.; Fiorica, C.; Pitarresi, G.; Puleio, R.; Tamburello, A.; Loria, R.; Giammona, G. Hyaluronic Acid Derivative with Improved Versatility for Processing and Biological Functionalization. *Macromol. Biosci.* **2016**, *16*, 1485−1496.
(24) Mun, E. A.; Morrison, P. W. J.; Williams, A. C.; Khutoryanskiy, V. V. On the Barrier Properties of the Cornea: A Microscopy Study of the Penetration of Fluorescently Labeled Nanoparticles, Polymers, and Sodium Fluorescein. *Mol. Pharmaceutics* **2014**, *11* (10), 3556−3564.
(25) Li, J.; Li, Z.; Zhou, T.; Zhang, J.; Xia, H.; Li, H.; He, J.; He, S.; Wang, L.; Yao, L.; Liang, D.; Zhu, L. Positively charged micelles based on a triblock copolymer demonstrate enhanced corneal penetration. *Int. J. Nanomed.* **2015**, *10*, 6027−6037.
(26) Shamsi, F. A.; Chaudhry, I. A.; Boulton, M. E.; Al-Rajhi, A. A. L-carnitine protects human retinal pigment epithelial cells from oxidative damage. *Curr. Eye Res.* **2007**, *32*, 575−584.
(27) Garrett, Q.; Xu, S.; Simmons, P. A.; Vehige, J.; Flanagan, J. L.; Willcox, M. D. Expression and localization of carnitine/organic cation transporter OCTN1 and OCTN2 in ocular epithelium. *Invest. Ophthalmol. Visual Sci.* **2008**, *49*, 4844−4849.
(28) Xu, S.; Flanagan, J. L.; Simmons, P. A.; Vehige, J.; Willcox, M. D.; Garrett, Q. Transport of L-carnitine in human corneal and conjunctival epithelial cells. *Mol. Vis.* **2010**, *16*, 1823−31.
(29) Siedlecki, J.; Wertheimer, C.; Wolf, A.; Liegl, R.; Priglinger, C.; Priglinger, S.; Eibl-Lindner, K. Combined VEGF and PDGF inhibition for neovascular AMD: anti-angiogenic properties of axitinib on human endothelial cells and pericytes in vitro. *Graefe's Arch. Clin. Exp. Ophthalmol.* **2017**, *255*, 963−972.
(30) Carneiro, Â.; Falcão, M.; Pirraco, A.; Milheiro-Oliveira, P.; Falcão-Reis, F.; Soares, R. Comparative effects of bevacizumab,

DOI: 10.1021/acs.molpharmaceut.8b00620
Mol. Pharmaceutics 2018, 15, 5031−5045

ranibizumab and pegaptanib at intravitreal dose range on endothelial cells. *Exp. Eye Res.* **2009**, *88*, 522−527.
(31) Palumbo, F. S.; Pitarresi, G.; Albanese, A.; Calascibetta, F.; Giammona, G. Self-assembling and auto-crosslinkable hyaluronic acid hydrogels with a fibrillar structure. *Acta Biomater.* **2010**, *6*, 195−204.
(32) Fields, R. the Rapid Determination of Amino Groups with TNBS. *Methods Enzymol.* **1972**, *25*, 464−468.
(33) Craparo, E. F.; Teresi, G.; Bondi', M. L.; Licciardi, M.; Cavallaro, G. Phospholipid-polyaspartamide micelles for pulmonary delivery of corticosteroids. *Int. J. Pharm.* **2011**, *406*, 135−144.
(34) Gao, J.; Ming, J.; He, B.; Fan, Y.; Gu, Z.; Zhang, X. Preparation and characterization of novel polymeric micelles for 9-nitro-20(S)-camptothecin delivery. *Eur. J. Pharm. Sci.* **2008**, *34*, 85−93.
(35) Di Prima, G.; Saladino, S.; Bongiovì, F.; Adamo, G.; Ghersi, G.; Pitarresi, G.; Giammona, G. Novel inulin-based mucoadhesive micelles loaded with corticosteroids as potential transcorneal permeation enhancers. *Eur. J. Pharm. Biopharm.* **2017**, *117*, 385−399.
(36) Kawazu, K.; Oshita, A.; Nakamura, T.; Nakashima, M.; Ichikawa, N.; Sasaki, H. Transport of acebutolol through rabbit corneal epithelium. *Biol. Pharm. Bull.* **2006**, *29*, 846−849.
(37) Civiale, C.; Licciardi, M.; Cavallaro, G.; Giammona, G.; Mazzone, M. G. Polyhydroxyethylaspartamide-based micelles for ocular drug delivery. *Int. J. Pharm.* **2009**, *378*, 177−186.
(38) Chu, Y.; Chen, N.; Yu, H.; Mu, H.; He, B.; Hua, H.; Sun, K. Topical ocular delivery to laser-induced choroidal neovascularization by dual internalizing RGD and TAT peptide-modified nanoparticles. *Int. J. Nanomed.* **2017**, *12*, 1353−1368.
(39) Pescina, S.; Sala, M.; Padula, C.; Scala, M. C.; Spensiero, A.; Belletti, S.; Gatti, R.; Novellino, E.; Campiglia, P.; Santi, P.; Nicoli, S.; Ostacolo, C. Design and synthesis of new cell penetrating peptides: Diffusion and distribution inside the cornea. *Mol. Pharmaceutics* **2016**, *13*, 3876−3883.
(40) Bongiovì, F.; Di Prima, G.; Palumbo, F. S.; Licciardi, M.; Pitarresi, G.; Giammona, G. Hyaluronic Acid-Based Micelles as Ocular Platform to Modulate the Loading, Release, and Corneal Permeation of Corticosteroids. *Macromol. Biosci.* **2017**, *17*, 1700261.
(41) Aliabadi, H. M.; Elhasi, S.; Mahmud, A.; Gulamhusein, R.; Mahdipoor, P.; Lavasanifar, A. Encapsulation of hydrophobic drugs in polymeric micelles through co-solvent evaporation: The effect of solvent composition on micellar properties and drug loading. *Int. J. Pharm.* **2007**, *329*, 158−165.
(42) Grimaudo, M. A.; Pescina, S.; Padula, C.; Santi, P.; Concheiro, A.; Alvarez-Lorenzo, C.; Nicoli, S. Poloxamer 407/TPGS Mixed Micelles as Promising Carriers for Cyclosporine Ocular Delivery. *Mol. Pharmaceutics* **2018**, *15*, 571−584.
(43) Mackie, A. R.; Goycoolea, F. M.; Menchicchi, B.; Caramella, C. M.; Saporito, F.; Lee, S.; Stephansen, K.; Chronakis, I. S.; Hiorth, M.; Adamczak, M.; Waldner, M.; Mørck Nielsen, H.; Marcellonic, L. Innovative Methods and Applications in Mucoadhesion Research. *Macromol. Biosci.* **2017**, *17*, 1−32.
(44) Rossi, S.; Ferrari, F.; Bonferoni, M. C.; Caramella, C. Characterization of chitosan hydrochloride-mucin interaction by means of viscosimetric and turbidimetric measurements. *Eur. J. Pharm. Sci.* **2000**, *10*, 251−257.
(45) Pitarresi, G.; Tripodo, G.; Cavallaro, G.; Palumbo, F. S.; Giammona, G. Inulin-iron complexes: A potential treatment of iron deficiency anaemia. *Eur. J. Pharm. Biopharm.* **2008**, *68*, 267−276.
(46) Al-Hadiya, B. M. H.; Bakheit, A. H. H.; Abd-Elgalil, A. A. Imatinib Mesylate. *Profiles Drug Subst., Excipients, Relat. Methodol.* **2014**, *39*, 265−297.
(47) Horvát, G.; Budai-Szűcs, M.; Berkó, S.; Szabó-Révész, P.; Soós, J.; Facskó, A.; Maroda, M.; Mori, M.; Sandri, G.; Bonferoni, M. C.; Caramella, C.; Csányi, E. Comparative study of nanosized cross-linked sodium-, linear sodium- and zinc-hyaluronate as potential ocular mucoadhesive drug delivery systems. *Int. J. Pharm.* **2015**, *494*, 321−328.
(48) Pescina, S.; Govoni, P.; Potenza, A.; Padula, C.; Santi, P.; Nicoli, S. Development of a convenient ex vivo model for the study of the transcorneal permeation of drugs: Histological and permeability evaluation. *J. Pharm. Sci.* **2015**, *104*, 63−71.
(49) Aulton, M. E. *Aulton's Pharmaceutics*; Harcourt Publishers Limited: London, 2013. DOI: 10.1007/s13398-014-0173-7.2.

DOI: 10.1021/acs.molpharmaceut.8b00620
Mol. Pharmaceutics 2018, 15, 5031−5045